THE DETECTION OF WETLANDS USING REMOTE SENSING IN QOQODALA, EASTERN CAPE

LESLEY ANNE GIBSON

Thesis presented in fulfilment of the requirements for the degree of Master of Applied Science at the University of Cape Town.

School of Architecture, Planning and Geomatics

Faculty of Engineering and the Built Environment

Supervisor: Dr. U. Rivett

August 2003

DECLARATION

I hereby declare that this is my own work, that the work of others is accurately reported and that this thesis has not been submitted in any form for evaluation to another university.

Signature removed

Lesley Anne Gibson

ABSTRACT

This dissertation aims to establish the possibilities of mapping wetlands in Qoqodala, Eastern Cape Province, South Africa, using Landsat and/or Aster imagery. The methodology for mapping wetlands using Landsat imagery, proposed by Thompson, Marneweck, Bell, Kotze, Muller, Cox and Smith (2002) is adapted and applied to the study area. The same methodology is modified for use with Aster imagery and applied to the study area. In addition, the possibilities of treating Aster as a hyperspectral image are investigated, and a methodology using hyperspectral processing techniques is implemented.

The results show that the methodologies chosen were unsuccessful in mapping wetlands in Qoqodala. The wetlands in the study area are typically small seeps and these entities are too small to be detected using the chosen imagery. In addition, the scene characteristics inhibit the classification of the image as the landscape in the study area is heterogeneous and this reduces classification accuracies. Finally, the seeps are spectrally too similar to the surrounding vegetation to be separated when classifying an image.

It is possible, that if the methodologies used in this study are applied to a different area, they may be successful. However in order to map wetlands in the study area, alternative techniques are recommended.

"It is a capital mistake to theorize before one has data.
Insensibly one begins to twist facts to suit theories,
instead of theories to suit facts."

Sherlock Holmes, 1888

ACKNOWLEDGEMENTS

The author wishes to acknowledge and thank the people and organizations who made this research possible.

Thank you to The Council for Geoscience and the Water Research Commission for funding this research. Thank you to The Council for Geoscience for allowing me the study leave which enabled the timely completion of the dissertation.

Thank you to my supervisor, Dr Rivett for her advice, encouragement and for the reviewing of the dissertation.

Thank you to Dr Luc Chevallier for his encouragement and for motivating me to carry on with the research even though the results were not the results I had hoped for.

Thank you to Dr S. Chevral of the BRGM in Orleans, France, for allowing me to visit and make use of their equipment. Thank you Dr Chevral for your time and ideas.

Thank you to Henk Coetzee for his suggestions and help with hyperspectral processing.

Thank you to my mother, Sheila Morrison for proof reading the document and correcting my English. Thank you to my husband, Michael, for his support throughout the course of this research.

TABLE OF CONTENTS

LIST OF FIGURES

LIST OF TABLES

CHAPTER 1

INTRODUCTION

This research project forms part of a larger research project funded by the Water Research Commission (WRC). The WRC project is entitled 'Hydrogeology of Fractured-Rock Aquifers and Related Ecosystems within the Qoqodala Dolerite Ring and Sill Complex, Great Kei Catchment' and is a joint venture by the Council for Geoscience, SRK Consulting, the University of the Western Cape and the Department of Water Affairs and Forestry.

The aims of the WRC project are to assess the occurrence of groundwater associated with the dolerite rings and sills in the Eastern Cape and to determine the relationship between ecosystems and groundwater in the study area. The techniques being utilised for the research include morphological and 3D analysis; hydrocensus of springs and boreholes; study of drainage systems; explorative drilling; detailed study of the ecosystem of springs; spatial analysis and remote sensing.

In order to understand the hydrogeological functioning of the study area and the influence of groundwater on ecosystems, it was necessary to know the location and occurrence of any springs, seepages or wetlands in the study area. The purpose of this part of the research project was to develop a method for mapping wetlands in the study area making use of remote sensing techniques.

It is assumed that the reader has a basic understanding of remote sensing and Geographic Information System principles, as these are not explained in the text. Appendix A contains a general introduction to remote sensing principles and interested readers can refer to this.

CHAPTER 2

OBJECTIVES

The objective of this research is to establish the possibilities of mapping wetlands in Qoqodala using Landsat and/or Aster Imagery.

The objective can be broken down into three minor objectives:

1. The methodology for mapping wetlands using Landsat imagery, proposed by Thompson, Marneweck, Bell, Kotze, Muller, Cox and Smith (2002), will be investigated. The methodology will be adapted and applied to the study area.

2. The methodology proposed by Thompson et al. (2002) will be modified for use with Aster imagery. The modified methodology will be applied to the study area.

3. A methodology to process an Aster image as a hyperspectral image, will be proposed. The methodology will be applied to the study area.

CHAPTER 3

DESCRIPTION OF STUDY AREA

3.1. Location

The study area is located approximately 15 kilometres north of Queenstown in the Emalahleni Municipality, Eastern Cape Province in South Africa (Figure 1). It covers an area of just over 20 000 km^2, the tribal land is known as Qoqodala and it is situated within the former homeland of the Transkei.

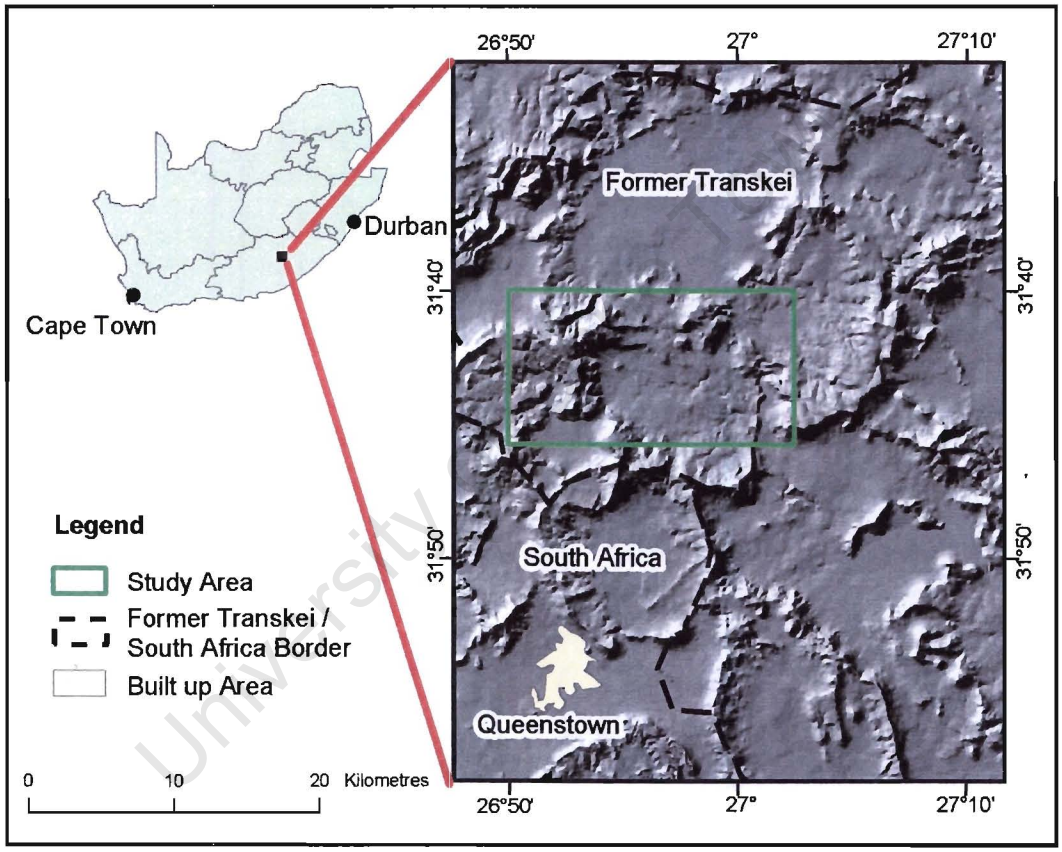

Figure 1: Location of the study area

3.2. Geology and Hydrogeology

On a regional scale, the geology of the area is characterized by dolerite sills, rings and

dykes which intruded into the Main Karoo Basin approximately 180 million years ago (Woodford and Chevallier, 2001). The Main Karoo Basin consists of sandstone, mudstone and shale of the Beaufort Group and the Elliot, Molteno, Dwyka and Ecca Formations. The location of these geological units is shown in Figures 2A and 2B with the distribution of dolerite dykes being shown in Figure 2A, and the dolerite sills being shown in Figure 2B.

The dolerite rings, sills and dykes were responsible for the formation of numerous shallow and deep fractured rock aquifers in the Karoo basin (Woodford and Chevallier, 2001). The dolerite caused many fractures in the host rock upon intrusion and on cooling jointing occurred in the dolerite. These fractures and joints are conduits and storage places for groundwater and are known as the deep fractured rock aquifers which are mentioned in the text.

The dolerite rings, sills and dykes control, to a large extent, the drainage pattern and influence the occurrence of many springs and seepages. Sills and rings of the Eastern Cape display a "ring within a ring" pattern. This pattern resulted in the vertical stacking of the dolerite which can be seen in Figure 2C. According to Chevallier, Goedhart & Woodford (2001), the vertical stacking of dolerite sills plays an important role in the concept of hydrostratigraphy, therefore the natural "basin" shape at the surface of the sill should be conducive to the establishment of individual ecosystems.

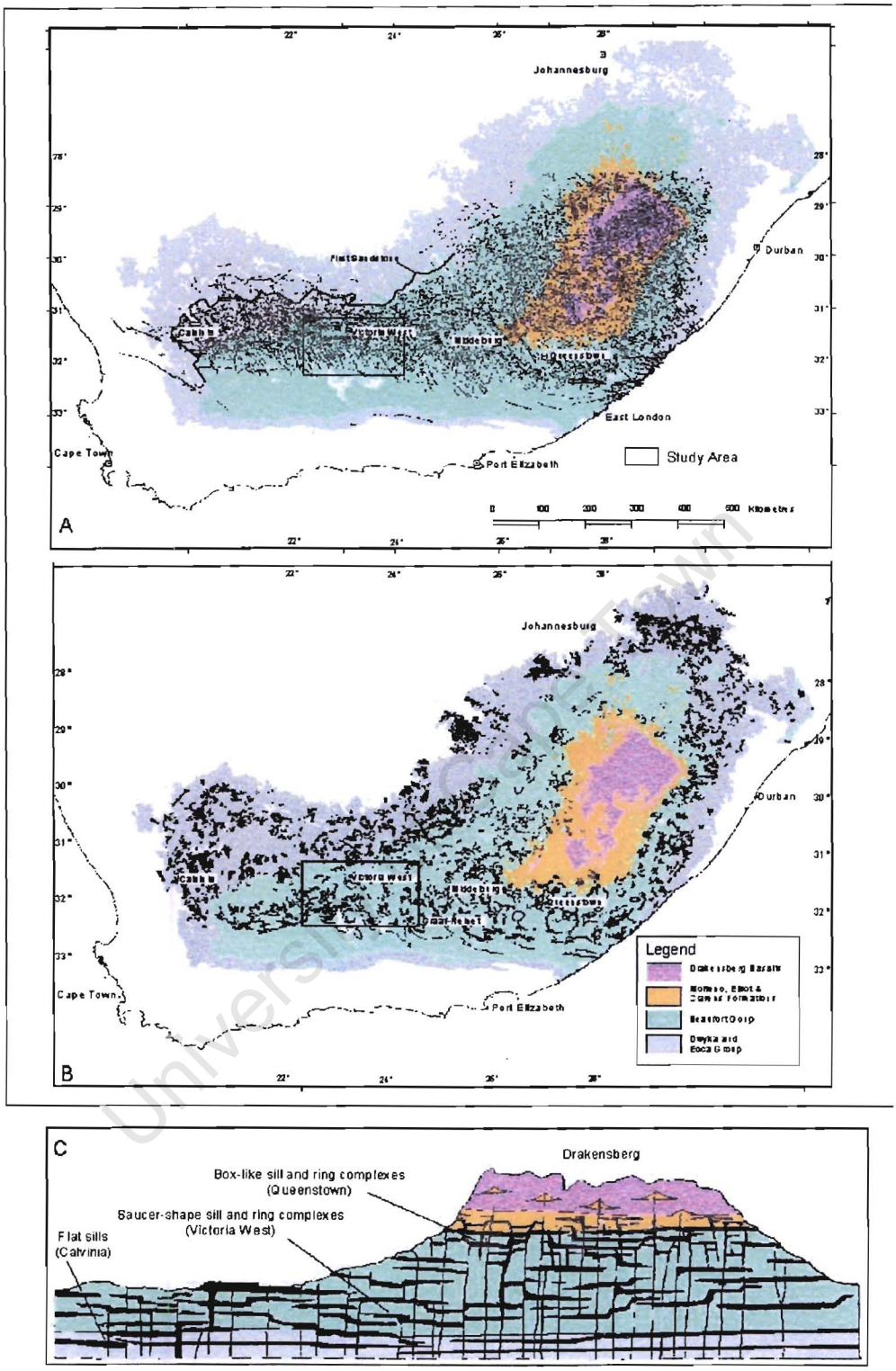

Figure 2: The distribution of dolerite dykes (2A) and sills (2B) in the Main Karoo Basin and the vertical stacking of the dolerite (2C). The study area used for the study in the Western Karoo is shown by the box in 2A and 2B. Adapted from Chevallier et al. (2001)

Two Water Research Commission projects investigating the hydrogeology of these fractured rock aquifers have already been carried out in the Western Karoo (Chevallier et al., 2001 and Woodford & Chevallier, 2001). Chevallier et al. (2001) concluded that the dolerite dykes and sills of the Karoo are structures conducive to the formation of deep-seated fractured-rock aquifers. The increase in yield with depth could also indicate that even higher yielding fractures may exist at greater depth (Woodford & Chevallier, 2001). A theoretical hydro-morpho-tectonic model of a dolerite ring was developed through this research and is illustrated in Figure 3. Interested readers are referred to Woodford & Chevallier (2001) for a detailed explanation of this model.

The geology of the study area is similar to that of the Western Karoo (Figure 2) and therefore it can be assumed that the geohydrology and the occurrence of groundwater will be similar. However the rainfall is greater in the present study area than in the Western Karoo and therefore the potential for groundwater recharge is greater.

The study area itself includes most of the Qoqodala Ring and a portion of the Zingqutu Ring. Figure 4 illustrates the location of the study area within the context of the dolerite outcrops. The circular flat inner sill surrounded by the elevated circular ring can be observed in Figure 5. This confirms the hydro-morpho-tectonic model proposed by Woodford & Chevallier (2001) shown in Figure 3.

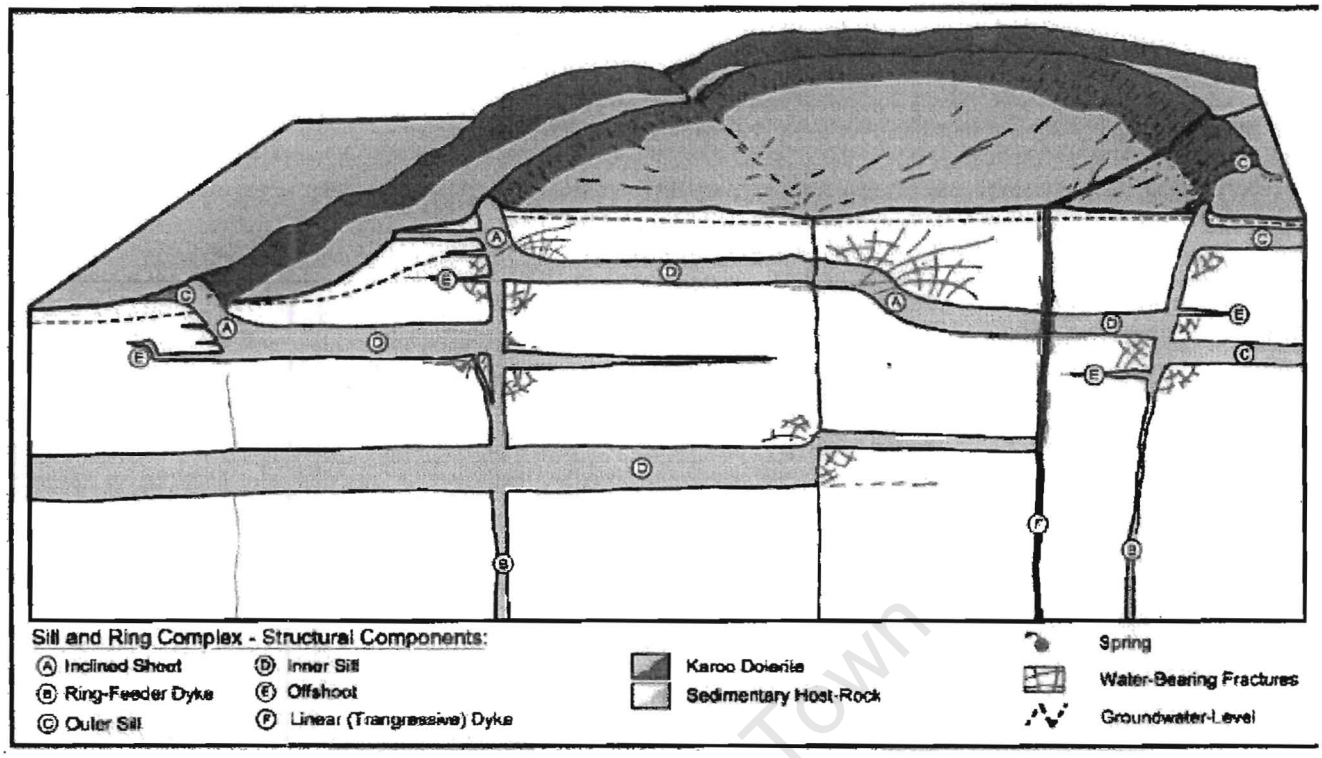

Figure 3: Conceptual hydro-morpho-tectonic model of a dolerite ring (Chevallier et al., 2001.)

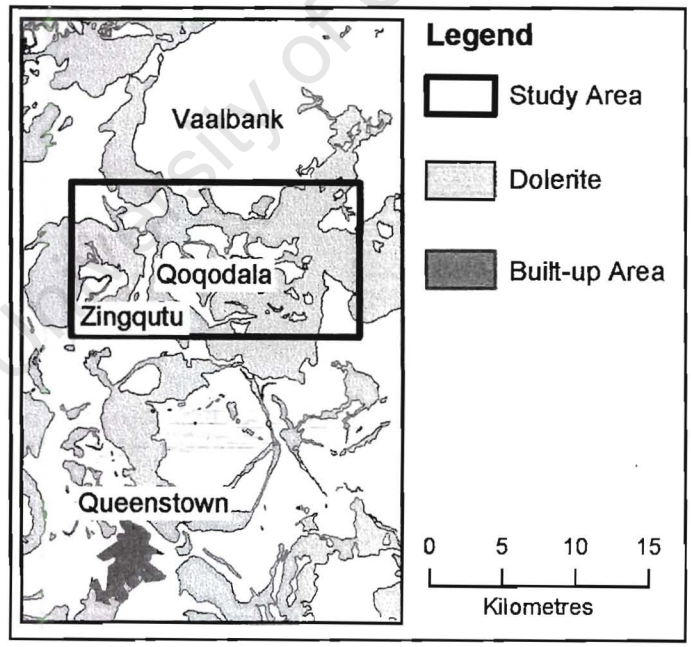

Figure 4: Distribution of dolerite in the region

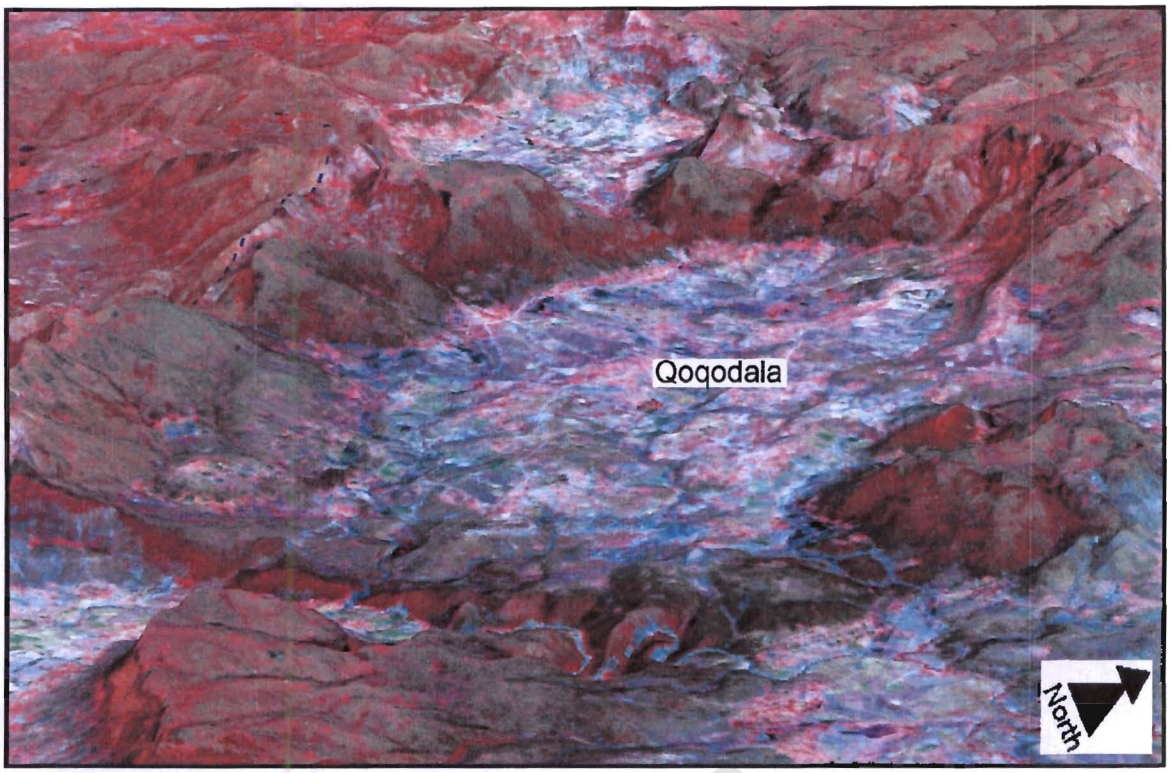

Figure 5: 3D Aster view of the Qoqodala Ring

3.3. Physiography and Climate

The landscape of the study area is influenced, to a very large extent, by the dolerite rings. The influence of the geology on the landscape is well illustrated in Figure 5 where the circular, elevated topography caused by the rings is apparent. It is clear that the distribution of the dolerite outcrop controls the topography, the climate, hydrology and the settlement and human activity patterns in the area. The elevation ranges from approximately 1000m above sea-level at the lowest point in the South East, to almost 2000m in the mountains in the North West.

The rainfall is seasonal with most precipitation occurring in the summer months. Figure 6 shows climatic data that is taken from the South African Atlas of Agrohydrology and Climatology (Schultz, Maharaj, Lynch, Howe & Melvil-Thompson, 2002). The mean annual precipitation is approximately 600mm. The temperature ranges from below 0°C at

night during the winter months to 40°C during the day in summer. The mean annual temperature is given as 15°C.

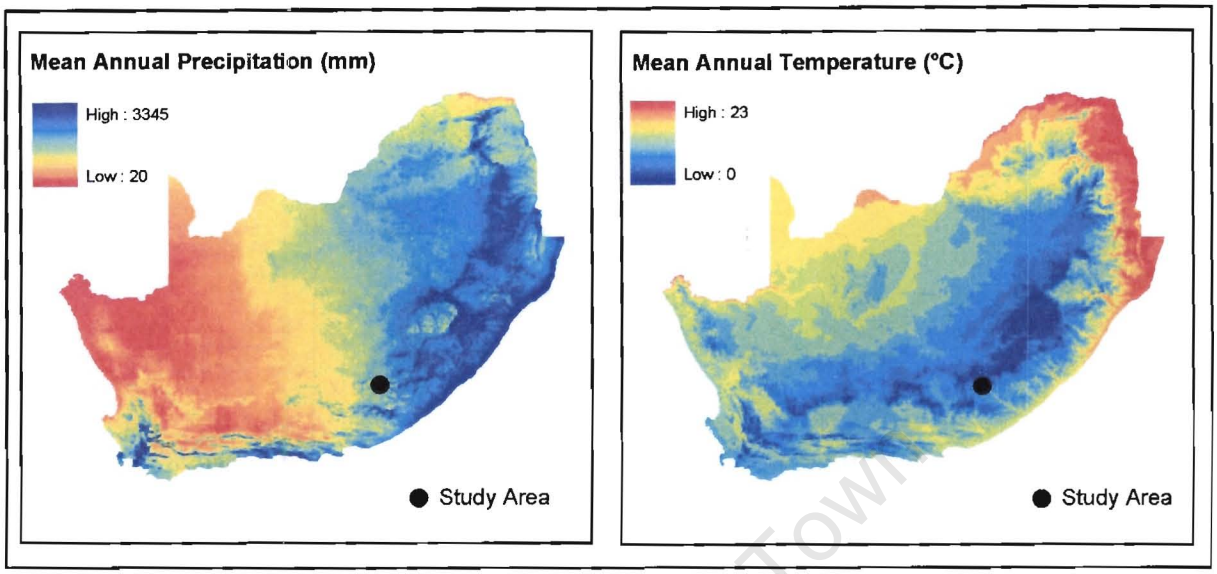

Figure 6: Location of the study area within the context of the climate of South Africa. Maps created from data obtained from the South African Atlas of Agrohydrology and Climatology (Schultz et al., 2002)

3.4. Human Activities

Qoqodala is situated in the former Transkei where poverty is widespread. According to Census 1996 data for Qoqodala, 80% of the population is unemployed, 24% is illiterate and less than one percent of households is supplied with piped water (Statistics South Africa, 2001). From these figures it is obvious that there is great need for all types of services and not just water supply. The National Water Act of 1998 states the size of the water resource (the reserve) must be known before water is allocated for any use. This is one of the main reasons for this research and is discussed in more detail in Chapter 4.

Most settlement occurs at the base of the slope of the dolerite rings. Agricultural activity in the form of subsistence farming and cattle grazing occurs on the predominantly flat sediments of the inner ring. Overgrazing and trampling are widespread, the fields of

crops are very small, the landscape is traversed by cattle trails and human paths and dwellings are isolated. Typical dwellings in the area can be seen in Figure 7.

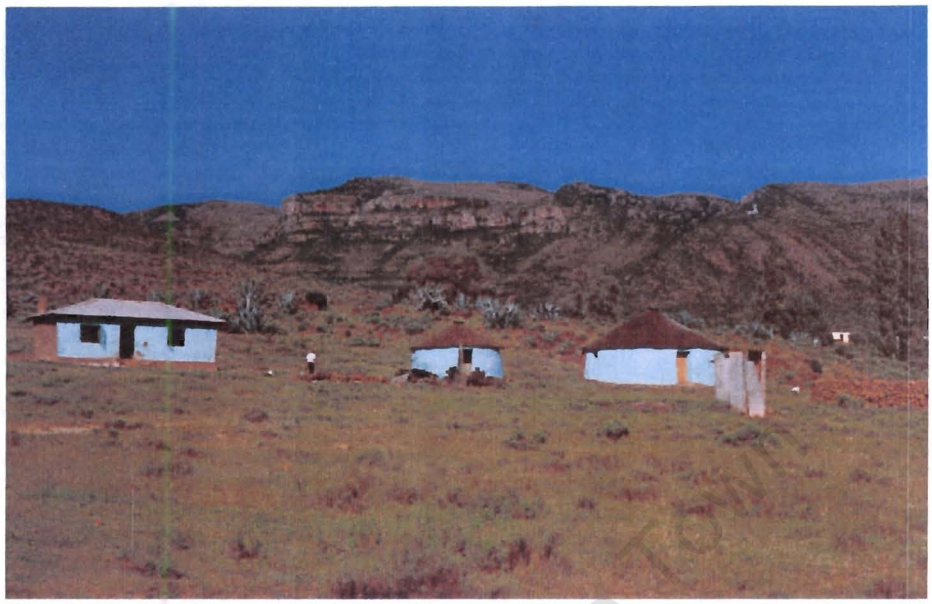

Figure 7: Typical dwellings in Qoqodala. Photograph courtesy of Dr L.P.Chevallier

3.5. Wetlands

An initial field trip in July 2002 revealed seeps located on the slopes of the dolerite above the settlement areas. A seep, which is classified as a type of wetland, is defined as: "An area, generally small, where water [sic] percolates slowly to the land surface....used by some for flows too small to be considered springs" (Bates & Jackson, 1980).

The characteristics of the seeps found in the study area were somewhat unexpected. It is normally assumed that the presence of green vegetation indicates the presence of water. However, in Qoqodala, the vegetation in the vicinity of the seep consists of grass which is dry, dead or dormant, whereas further away, the vegetation consists of greener shrubs and succulent bushes (Figure 8).

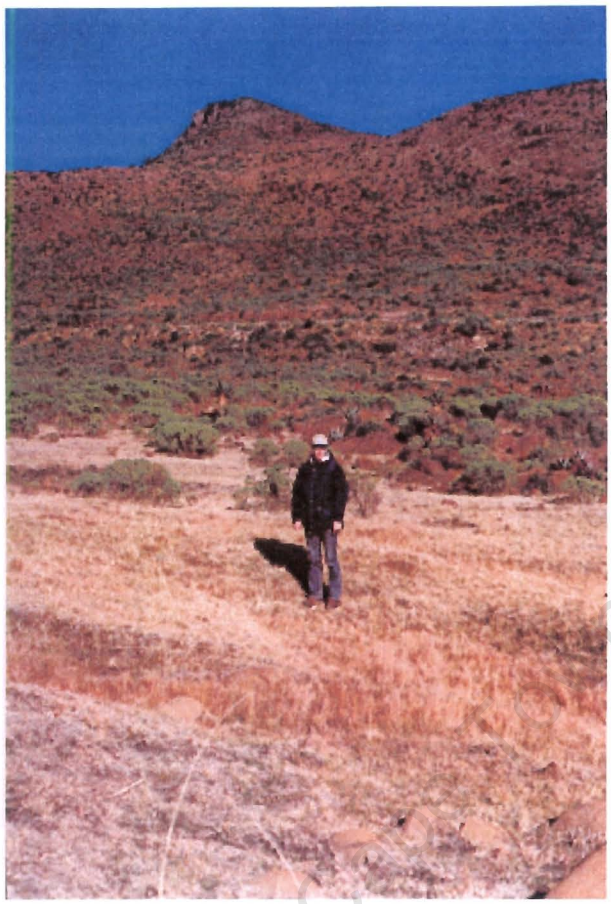

Figure 8: A seep in the study area. The seep is located to the right and in front of the author. Photography courtesy of Dr L. P. Chevallier

It is surmised that in the area immediately surrounding the seep, the water table is high and in the wet season after rain, the water table would be very close to the surface. The hardy shrubs, adapted to harsher, more arid conditions, are unable to grow and the grass and wetland vegetation thrive.

Wetland plants could not always be identified in the immediate vicinity of the seeps. However this does not imply that wetland vegetation is not present, as the vegetation on the seeps is grazed extensively by cattle, so the grass and other vegetation were cropped short making identification very difficult. In spite of this, a type of sedge, which is a typical wetland plant, was identified in the vicinity of some of the seeps. Furthermore, the seeps were characterized by dark organic and peaty soils in which mud cracks were apparent in the dry season. This indicates that these areas are saturated for at least some

part of the year. The seeps also seem to occur in small depressions, which could be the start of future valleys. The individual seeps were typically smaller than $40m^2$ and sometimes as small as about $9m^2$. In addition, the seeps tend to occur in zones (Figure 9) of varying size and quantity.

Figure 9: **A zone of seeps**

CHAPTER 4

BACKGROUND TO RESEARCH

The subject of water is becoming an increasingly important issue around the globe, whether it be too much of it in the form of floods, too little of it in the form of droughts or polluted water resources or disputes between countries who share it. South Africa is no exception to this trend.

In the past dams were seen to hold the answer to the world's water supply needs. However it is becoming increasingly obvious that although dams may address immediate needs, the negative impacts cannot be ignored. These impacts are complex, varied and often profound in nature. In many cases dams have led to irreversible loss of species, populations and ecosystems. (World Commission on Dams, 2000)

South Africa is a water stressed country where water planners and managers are faced with increasingly complex issues. The South African Yearbook, published by Government Communications, describes South Africa as follows: "The country is largely semi desert and prone to erratic, unpredictable extremes in the form of droughts and floods. Apart from erratic rainfall and the low ratio of run-off (which affects the reliability and variability of river flow) the average potential evaporation is higher than the rainfall in all but a few isolated areas where rainfall exceeds 1400mm per year." (SA Yearbook, 2003)

Not only is the rainfall - and therefore the water resources - of the country unevenly distributed, so too is the population. The majority of the population is found in one of two situations. Either concentrated in the metropolitan areas; or highly scattered in the rural areas. Both environments have their challenges.

South Africa is rapidly urbanising and for the past fifteen years there has been a phenomenal increase of population in the major cities which has led to an increased demand for water in these areas. Metropolitan Councils are continuously investigating

ways of meeting the rising demands and have been considering options such as the building of new dams and exploring the potential of using ground water to supplement the water supply.

The problems in the rural areas are very different but equally challenging. South Africa's political past has created many inequalities and this is very apparent in the rural areas. Covering a large portion of the South African countryside are large, traditionally white, commercial farms. In the past, these commercial farmers received government subsidies and the farmers were well supported by the Department of Water Affairs in terms of their water supply, which is mostly in the form of small dams and boreholes. These farms were also supplied with electricity, which enabled the operation of electric boreholes. At the opposite end of the political spectrum were the so-called black homelands. These rural areas consisted of tribal land where the people existed as subsistence farmers. There was very little support from government in terms of water or electricity supply and these farmers were almost entirely reliant upon rain for irrigation of their crops. Political change in South Africa has highlighted these past inequalities and government is committed to righting past wrongs (Asmal, 1999). For this purpose, the Water Services Act of 1997 and the National Water Act of 1998 were passed.

Groundwater, despite its relatively small contribution to bulk water supply (13%), is an important and strategic water resource in South Africa. Owing to the lack of perennial rivers in the semi-desert and desert regions of the country, two thirds of South Africa's surface area is largely dependent on groundwater. Through the Government's commitment to meeting basic water needs of communities, groundwater has also become a strategic resource for village water supply in the wetter parts of the country, because of its availability and effectiveness in widely scattered small-scale user situations. (Vegter, 2001)

The National Water Act states that the reserve of a water resource must be determined before that resource can be allocated for use. The reserve is made up of two components, the human reserve and the ecological reserve. The basic human need reserve is that

portion of the reserve which provides for the essential needs of individuals served by the water resource and includes drinking water. The ecological reserve relates to the water required to protect the aquatic ecosystems of the water resource (National Water Act, 1998).

The necessity of the calculation of reserve has opened a new door as far as research is concerned in South Africa. Groundwater reserve has traditionally been very difficult to calculate and as the groundwater reserve is considered part of the reserve, it has stimulated innovative new research in this field. The mapping of wetlands has become a priority as wetlands are closely linked to groundwater recharge as well as the release of groundwater into the surface water flow. Wetlands help regulate water flow by slowing it down in times of heavy rain, absorbing the water like a sponge and then slowly releasing it. It is for this reason that the location and extent of wetlands must be known when calculating groundwater reserve.

There is no existing spatial data wetland inventory in South Africa, so wetlands needed to be mapped for the study area. The properties of multi-spectral satellite imagery are such that they contain bands that fall outside the wavelengths visible to the human eye. For example, wavelengths in the near infrared are very useful for vegetation mapping and these properties make it a more desirable mapping medium than colour or black and white aerial photography. Multi-spectral satellite imagery (see Appendix A) is recognized as being a very cost effective method of producing land cover maps at a regional scale and as wetland mapping can be seen as a form of land cover mapping, it was the chosen method for this research. It is assumed that the reader is familiar with basic remote sensing concepts, as these will not be explained in the text. However, Appendix A can be consulted for a brief overview of remote sensing principles, while details of Landsat and Aster imagery can be found in Appendix B.

CHAPTER 5

LITERATURE REVIEW AND DISCUSSION OF RELEVANT THEORY

5.1. Literature Review

The principle aim of this research project is to map wetlands using remote sensing techniques. It was observed during fieldwork (Chapter 3.5) that the wetlands in the study area are little more than seeps. Although an extensive literature search was carried out, only one previous study on the subject of mapping seeps or springs using remotely sensed images was discovered. Saraf, Goyal, Negi, Roy & Choudhary (2000) used a combination of remote sensing and spatial analysis using Geographic Information Systems (GIS) to delineate springs in a mountainous region in India. However GIS featured more strongly than remote sensing, as the satellite images were specifically used to produce land use maps and to map lineaments. Because of the lack of literature relating to spring or seepage mapping, it became necessary to broaden the subject of the literature search to incorporate the mapping of wetlands using remote sensing. This is an acceptable topic on which to conduct a literature search as seeps are a type of wetlands (see Chapter 3.4).

The literature on this topic is much more extensive and numerous examples were found. Thompson (1996) defined wetlands as: "natural or artificial areas where the water level is at (or very near) the land surface on a permanent or temporary basis, typically covered in herbaceous or woody vegetation cover". This definition is taken from a paper in which Thompson proposed a standard hierarchical scheme for the classification of remotely sensed data designed to suit the South African environment. The framework is based on known land cover classes that can be derived from high-resolution remotely sensed data such as SPOT, Landsat TM and today would include Landsat ETM+ and Aster data. Thompson tried, as far as possible, to take into account pre-existing classification systems or codes that had been used within various organisations.

Another South African example deals with the determination of the groundwater reserve for all or part of any significant water resource. The determination of the reserve has become essential with the introduction of the National Water Act in 1998. A generic method for determining the reserve is outlined in the Act. Conrad, Hughes & van der Voort (2000) undertook a study to assess the applicability of commercial multi-spectral data as a tool for determining the reserve. As this was a case study, only one Landsat TM image was used and for this reason the results should be interpreted with caution. The study entailed the mapping of geohydrological region types (under which springs and wetlands fall) using a Landsat TM image and GIS. For the identification of wetland areas, standard classification techniques were used and found to be successful. It was found that natural spring flow was difficult to assess directly from a satellite image. Conrad et al. (2000) suggested an alternative would be to use GIS analysis to identify areas of potential groundwater/ stream interaction using water level and topography. It was consequentially proposed that this should be supported using Landsat TM to identify areas of natural vegetation growth. The author proposes that a possible method of improving these results would be to use multiple scenes of the same image. Using this method, wet season images could be compared with dry season images and more detailed information could be extracted.

In a study by Whitman, Gubbles & Powell (1999), surface water bodies were mapped in order to be used as a data layer in a study which looked at the spatial interrelationships between lake elevations, water tables and sinkhole occurrences in Florida. The topic of study is irrelevant to this research, although the method used to extract surface water bodies deserves a mention. From the premise that surface water has a low reflectance in the middle infrared wavelengths, a band ratio was computed by dividing band 2 by band 5. The authors stated that this is an extremely robust way of mapping water bodies using Landsat imagery.

Frazier & Page (2000) set out to assess the accuracy of using Landsat TM data to locate and delineate water bodies. Single band density slicing and the multi-spectral maximum-likelihood algorithm were used to classify the satellite data. Density slicing is used to quantify the accuracy of using a single band to map water bodies. The more advanced multi-spectral classification was completed to give a benchmark result using all reflective bands for comparison with the density slicing classification. It was found that density slicing classification of the three visible bands substantially overestimates the area of water contained in an image. The infrared band classifications gave significantly better results with band 5 giving the best visual approximation result. Supervised maximum-likelihood classification produced the best overall results. However, for small pools (defined as having a depth of 0.2 - 2m and area of 0.005 - 3.2ha), maximum likelihood performed significantly worse than density slicing of band 5. Of concern is the percentage accuracy for small pools being the lowest, with a result of 48.2%.

A method which automatically detects water surfaces in Landsat images was developed by Castano et al. (2000) who proposed that an area should be taken to be a water surface if:

$$\frac{Band4}{Band3} - \frac{Band4}{Band5} \geq 0.4$$

As the data had a resolution of 30m, this was too coarse to detect small water channels or water under pheatophytic vegetation (reed beds). So yet again, the problem of resolution surfaced. Another concern raised was that when the water body is shallow, some pixels are misclassified.

One of the most applicable studies discovered in the search of the literature, was a study by Lunetta & Balogh (1999) concerning the applicability of Landsat TM imagery for wetland identification. Lunetta & Balogh (1999) began by selecting a Landsat image which coincided with a seasonally wet, leaf-on period. The premise that water absorbs energy in near infrared wavelengths was adopted. This should have resulted in lower

reflectance values in the infrared wavelengths for saturated (wetland) areas when compared to the drier upland (non-wetland) sites. The technique used was to divide the image into wetland and upland categories by applying grey-level thresholding to the infrared bands. Various density slicings of band 5 were visually interpreted until a brightness threshold separating wetlands from uplands was found. Visual analysis of the near infrared bands and band 7 revealed that band 5 best discriminated between dry and wet areas. It was also found that the use of multi-date imagery significantly improves the accuracy of wetland mapping. It should be noted that this study was carried out in a temperate mid-Atlantic region of the United States where conditions differ vastly from those in the Eastern Cape.

An interesting study was carried out by Dupigny- Giroux & Lewis (1999), in a semi-arid environment in north east Brazil. A method for working out the surface moisture index using bands 1, 3, 4, 5 & 6 was derived. The moisture index did not provide actual estimates of soil moisture, but instead, characterised wetness relative to other features within a given scene. A successful ratio was found to be band 4/band 5 when plotted against band 6. The explanation given for this was that band 1 is known for its water penetrating properties and is also used to differentiate between soil and vegetation. Band 4 has been widely used for its biomass determining features but also allows for separation between water bodies and vegetation. Band 6 is often used in vegetation stress analysis and soil moisture discrimination. Unfortunately the use of band 6 meant that all other bands had to be resampled to a resolution of 60m.

In a study in 1998, Arbuckle, Huryn & Israel concluded that high resolution data is needed for the mapping of upland bog formations and that SPOT data, although of adequate resolution, lacks the required spectral information. Munro & Touron (1996) demonstrated the suitability of Landsat TM for estimating marshland degradation in Southern Iraq. However, due to insufficient fieldwork, they admitted they were unable to assess the accuracy of their results.

There have been many more publications on the topic of wetland mapping using remote sensing. The reader is referred to the Reading List for a more complete review of the literature.

Within South Africa, the Department of Environment Affairs and Tourism (DEAT) has recognized the need to create an inventory of wetlands in order to effectively manage and conserve wetlands in South Africa. With this aim in mind, a pilot project (Thompson, Marneweck, Bell, Kotze, Muller, Cox & Smith, 2002) was commissioned to develop a methodology for establishing a cost-effective, accurate and comprehensive National Wetland Inventory. The remote sensing imagery chosen was multi-temporal Landsat TM and Landsat ETM+. Landsat was identified as having the best combination of spatial, spectral and costing characteristics when compared to other medium resolution satellite sensors. The study used a multi-temporal, multi-stage classification approach and attempted to map vegetated, as well as non-vegetated wetlands. Further details of the methodology proposed by Thompson et al. (2002) will be discussed in Chapter 6.1. as this methodology was selected for modification and use in this research project. The conclusion drawn by Thompson et al. (2002) on using Landsat imagery for wetland mapping was as follows:

1. Satellite based mapping is not suitable for detailed wetland mapping, if Landsat-type imagery is used, and the minimum mapping standards were as specified[1].
2. It would be possible to use an alternative form of satellite imagery to increase spatial resolution. However the cost of this is too high and therefore not a realistic alternative.
3. If higher mapping accuracies are desired, field work combined with aerial photography techniques are recommended.

[1]The terms of reference stated that the aim was to map 90 percent of all wetlands >1 ha and 50 percent of all wetlands >0.5 ha

4. Wetland mapping using Landsat imagery is essentially limited to a generic "presence or absence" mapping of "core" wetland areas (Thompson et al., 2002).

Thompson et al. (2002) also concluded that the mapping accuracy of open-water wetlands is generally much higher than that of vegetated wetlands. This is due to the fact that open-water wetlands differ spectrally to the surrounding land-covers far more than vegetated wetlands do. (Thompson et al., 2002)

5.2. Discussion of Relevant Theory

Should the reader wish to consult literature for an introduction to remote sensing principles, Mather (1999) is recommended. Alternatively, Appendix A outlines some basic principles and Appendix B can be referred to for detailed information on Landsat and Aster imagery. A discussion of image processing techniques which were used in the research and with which the reader may wish to become familiar in order to understand this thesis, now follows.

It may make reading easier to bypass this section at this stage and refer back to it as needed. When the techniques are mentioned later in the text, the relevant section in Chapter 5.2 is given to enable quick reference.

5.2.1. Principal Component Analysis (PCA)

The Principal Component Analysis is a standard method for deriving a new set of spectrally reduced images from the original image. It is based on the observation that adjacent bands in multi-spectral remote sensing images are visually and numerically similar which means they are generally correlated. This implies that there is a redundancy in the information contained in these bands. (Mather, 1999)

The process is a linear transformation that projects each image pixel spectrum to a new set of orthogonal coordinate axes. These axes are chosen so that the output images are uncorrelated and ordered by decreasing variance, with the first principal component axis corresponding to the direction of maximum variance in spectral space (Microimages, 2003). Mather (1999) illustrates and describes the correlations present between bands with the figure (Figure 10) and text below.

"Presume the plot below is a two band image data set, where a random sample of pixels has been plotted on a scattergram according to their digital numbers. Then it can be seen that Band X and Band Y are not perfectly correlated but there is a dominant direction of scatter (or variability) along line AB. If this dominant direction is chosen as the major axis then a minor axis (CD) could be drawn at right angles to it. A plot using the axes AB and CD rather than the conventional axes might prove more revealing of structures present within the data. If the variation in direction CD contains only a very small amount of the data, then it can be ignored without much loss in information. A two dimensional data set is thus reduced to one dimension."

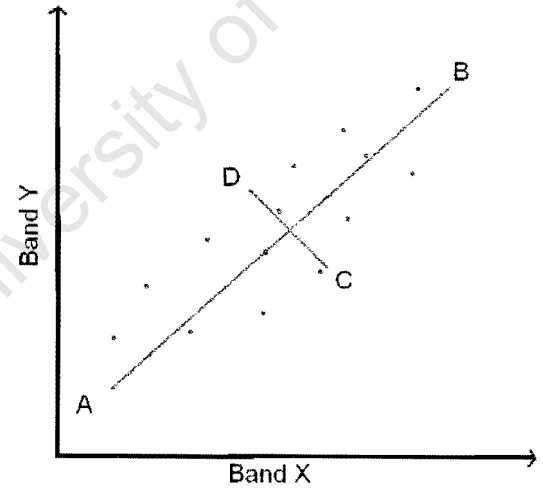

Figure 10: Scattergram. After Mather (1999)

If the same concept described above is applied to N-dimensional space, where each axis is represented by a multi-spectral band, the same dominant direction will be observed.

The dominant direction will then be represented by an axis which is the first principal component. The second principal component is orthogonal to the first and the third principal component is orthogonal to the second and third principal components. In this way, the axes and therefore the principal components are always uncorrelated.

In mathematical terms, PCA identifies the optimal linear combinations of the original bands which account for the variation of pixel values in an image. The linear combinations are given as

$$A = C_1X_1 + C_2X_2 + C_3X_3 + C_4X_4$$

where X_1, X_2, X_3, and X_4 are pixels in four spectral bands, and C_1, C_2, C_3, and C_4 are coefficients or eigenvalues[1], applied individually to the values of the respective bands. *A* represents a transformed value for the pixel. (Campbell, 1996)

Optimum values for eigenvalues are calculated in such a way that the values they produce account for maximum variation within the entire data set. Thus, this set of coefficients provides maximum information which can be conveyed by any single band formed by linear combination of the original bands (Campbell, 1996). The procedure for calculating the coefficients or eigenvalues is complex and will not be discussed in this thesis. The first three principal components typically contain 97% of total variance within a data set, with the first principal component containing approximately 70%.

5.2.2. Tasseled Cap Transformation

The tasseled cap transformation is based on the same principles as the principal component analysis. It is designed to rotate the axes in such a way that the data in which we are most interested is extracted. Where the tasseled cap transformation differs from

[1] Eigenvalues: a set of quantities, in *n*-dimensions, derived using linear algebra which defines the length of the principal axes of the ellipsoid which encloses scatterpoints on a scatter diagram. Eigenvalues are measured in units of variance (Mather, 1999) and the sum of the eigenvalues equals the sum of the band variances in the original image (Microimages, 2003).

principal component analysis is that in tasseled cap transformation the coefficients by which the axes are rotated, are predefined.

The transformation was first proposed in 1976 by Kauth and Thomas who found that in four dimensional MSS[1] data space, there is a line, oblique to all four axes, which represents soils, and a triangular area which represents various stages of growth in vegetation (Crist & Cicone, 1984).

The tasseled cap transformation defines a new rotated coordinate system in which the soil line and plane of vegetation are more clearly shown. The new axes of this coordinate system are termed brightness, greenness, yellowness and nonesuch. The first three indices namely; Brightness, Greenness and Yellowness, include most crop development information and have been useful in mapping crop development from bare soil through the greening process to maturity and harvest (Yuen, 1998). The coefficients, which determine the rotation of the axes, were obtained using samples from Illinois, USA, so whether the tasseled cap transformation can be used elsewhere is open to debate.

Crist & Cicone (1984) adapted the tasseled cap transformation for use with Landsat TM data. It was found that data in the six reflective bands occupy three dimensions. Two of these dimensions relate to the original Tasseled Cap Greenness and Brightness index; and the third component is affected mainly by the short wave infrared (SWIR[2]) bands.

This third dimension has been called Wetness, as absorption by vegetation in the mid-infrared bands is caused primarily by soil moisture content.

The influence of each Landsat TM band in the creation of the new indices is as follows:

- Brightness: a weighted average of the six Landsat TM bands

[1] MSS: Multi-spectral Scanner. Landsat satellite preceding Landsat TM. Landsat MSS consisted of only four spectral bands which explains the reference to four dimensional space.
[2] Short wave infrared is also known as mid infrared (MIR)

- Greenness: visible, near infrared (NIR) contrast with little contribution from mid infrared (MIR) - Bands 5 and 7.
- Wetness: contrast between MIR (bands 5 and 7) and the red and NIR (bands 3 and 4). Mather (1999)

5.2.3. Normalised Difference Vegetation Index

The following explanation is modified from Mather (1999) and Sabins (1997). The normalised difference vegetation index (NDVI) uses a ratio of the visible red and near infrared bands of an image to create a 'greenness' or biomass index. The NDVI can be applied to any satellite image which contains bands in the red and near infrared wavelengths. It is used on a global or continental scale using coarse resolution imagery to study patterns in vegetation change, and can be used on a more regional or local scale using Landsat or SPOT. The NDVI is based on the differences in reflectance by healthy vegetation of the visible red and near infrared wavelengths. The typical reflectance curve for vigorous vegetation (Figure 11) is well known and is found in many texts. In Figure 10, it can be clearly seen that there is a small peak in reflectance between 0.5 and 0.6μm. This corresponds to the green light part of the spectrum, and it is for this reason that vegetation appears green to the human eye. Typically, 70 – 90% of both blue and red light is absorbed by chlorophyll and other pigments in a leaf in order to provide energy for the process of photosynthesis. Reflectivity rises sharply in the near infrared wavelengths at 0.75μm and remains high until about 1.35μm. The reason for this reflectivity is a result of interaction between the internal leaf structure and electromagnetic radiation at these wavelengths. As a plant ages or becomes stressed, the first spectral change to take place is in the near infrared wavelengths. This change is not visible to the human eye, and for this reason, near infrared photography and satellite imagery are used in agriculture to detect early signs of stress in plants.

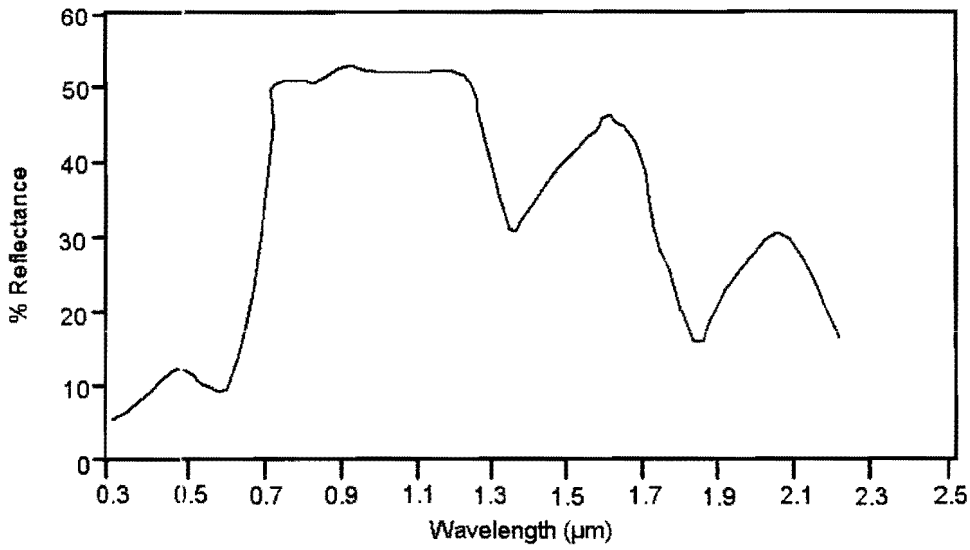

Figure 11: Idealised spectral reflectance curve for vigorous vegetation. After Mather (1999)

The normalized difference vegetation index (NDVI) exploits this reflectance curve. It is defined as:

$$NDVI = (NIR - R) / (NIR + R)$$

where NIR is the near infrared band and R is the visible red band. (Mather, 1999).

Values in the NDVI range from -1 to +1. Vegetated areas are generally indicated by higher values due to their high reflectance in the near infrared and low reflectance in the visible red wavelengths. Conversely, lower values indicate non-vegetated features such as water, barren land or clouds.

An advantage of using the NDVI over other more simple vegetation indices, is that it is an index which is a ratio of two bands. The value of dividing one band by another is to reduce the undesirable effects of noise, topography and differences in illumination as illustrated in Figure 12. The ratio of near infrared to red spectral bands is virtually identical at points A and B despite different levels of solar irradiation. Thus, using a ratio produces a result which can be used in a comparative study over time, or between regions. (Mather, 1999; Sabins, 1997)

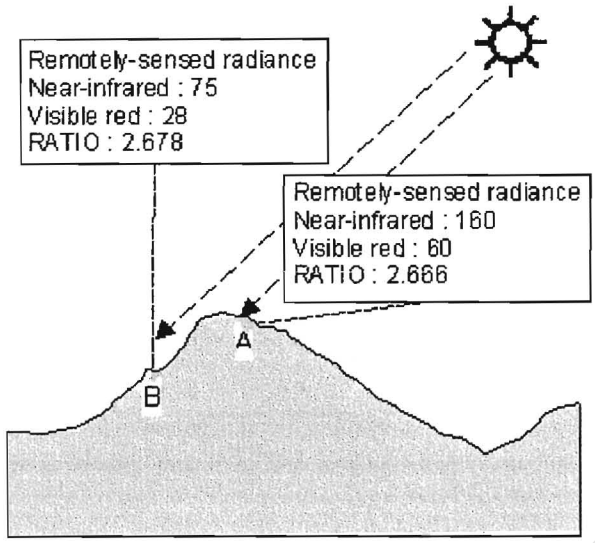

Figure 12: The ratio of bands reduces the effects of topography (Mather, 1999)

5.2.4. Image Classification

Descriptions of image processing techniques are found in many introductory texts to remote sensing. Campbell, 1996; Lillesand & Kiefer, 2000; and Mather 1999, were referred to and the following explanation is an adaptation of their texts.

The objective of spectral image classification procedures is to automatically categorize all pixels in an image into land cover classes or themes. Each pixel is treated as an individual unit composed of digital number (DN) values in several spectral bands. Different feature types (e.g. water bodies or forest) contain different combinations of DN based on the reflectance and emittance characteristics of that particular feature type. The number of DN values per pixel equals the number of spectral bands contained in the image file to be classified. The classification procedure compares pixels to each other - and in the case of supervised classification, to those of known identity - and then assembles groups of similar pixels into classes. These classes correspond to informational categories of interest to users of the remotely sensed data. In principle, the classes resulting from the classification are homogeneous i.e. pixels within a class are more

similar to pixels in a different class. However, in practice it is obvious that there will be variability within each class.

Spectral classification is usually separated into two categories; namely supervised and unsupervised classification. The fundamental difference between the two is that supervised classification involves a training step before the classification step. In the training step the user identifies areas on the image where the land cover is known. The spectral signatures of the known areas are then used to classify all other pixels in the image according to the input classes. In the case of unsupervised classification, the image data are first classified by aggregating them into natural spectral groups - known as clusters - present in the scene. The user then determines the land cover identity of these groups by comparing the classified image to ground reference data. (Campbell, 1996; Lillesand & Kiefer, 2000; and Mather, 1999).

As unsupervised classification was the classification method used in this research, a more detailed explanation follows. For the reader's interest, the advantages and disadvantages of each classification methodology can be found in Appendix C.

5.2.4.1. Unsupervised classification

The explanation which follows is modified from that of Lillesand & Kiefer (2000) and Research Systems, Inc. (2001). For a more mathematical explanation, Mather (1999) can be consulted.

Unsupervised classifiers do not use training data as the basis for classification; algorithms cluster pixels in a data set based on statistical relationships. These algorithms examine the pixels in an image and assign them to a class, based on the natural grouping or clustering of the digital number (DN) values. The basic premise is that values within a given cover type should be close together in measurement space, whereas data in different classes should be well separated.

Lillesand & Kiefer (2000) use the following example to illustrate this.

"...consider a two-channel data set. Natural spectral groupings in the data can be visually identified by plotting a scatter diagram. For example, in Figure 13 [sic] below, we have plotted pixel values acquired over a forested area. Three groupings are apparent in the scatter diagram. After comparing the classified image data with ground reference data, we might find that one cluster corresponds to deciduous trees, one to conifers and one to stressed trees of both types (indicated by D, C and S in the figure). In a supervised approach we may not have considered training for the 'stressed' class"

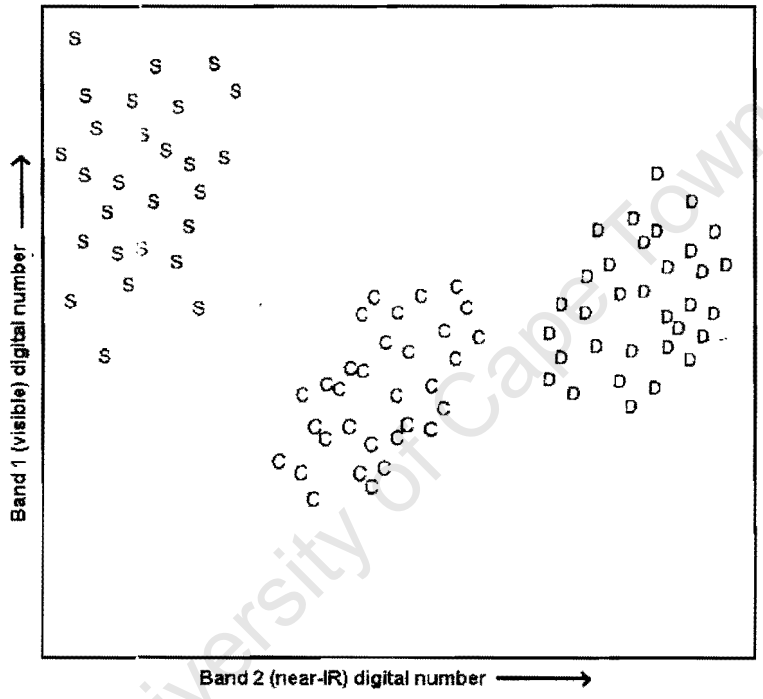

Figure 13: Spectral classes in two-channel data. Lillesand & Kiefer, 2000.

This example highlights the one of the advantages (see Appendix C) of using unsupervised classification, as the 'stressed' class may not have been initially apparent to the researcher.

Two of the most well known unsupervised classification methods are the K- means and the ISODATA classifiers. ISODATA classification is used in this research and a short

discussion follows. For explanations on K-Means classification, the following can be consulted: Mather (1999), Lillesand & Kiefer (2000) and Research Systems, Inc (2001).

ISODATA is an acronym derived from Iterative Self-Organising Data Analysis Technique, with a terminal 'A' added for aesthetic reasons (Mather, 1999). "ISODATA unsupervised classification calculates class means evenly distributed in the data space and then iteratively clusters the remaining pixels using minimum distance techniques. Each iteration recalculates means and reclassifies pixels with respect to the new means. Iterative class splitting, merging, and deleting are done based on input threshold parameters. All pixels are classified to the nearest class unless a standard deviation or distance threshold is specified, in which case some pixels may be unclassified if they do not meet the selected criteria. The process continues until the number of pixels in a class changes by less than the selected pixel change threshold or the maximum number of iterations is reached." (Research Systems, Inc, 2001).

5.2.5. Spectral mixture analysis

The following explanation on spectral mixture analysis (SMA) is adapted from the texts of Lillesand & Kiefer (2000) and Research Systems, Inc (2001).

SMA, also known as linear spectral unmixing, is used to determine the relative abundances of land cover types which are represented in a multi-spectral image based on the land cover types' spectral characteristics. It involves the comparison of the mixed spectral signatures contained in the image to a set of "pure" reference spectra. It is assumed that the spectral variation in a scene is caused by the varying mixtures of the land cover types or classes which are present in the image. The result is an estimate of the approximate proportions of the ground area of each pixel that is occupied by each of the land cover classes. The main advantage of using SMA is that it provides useful information at the subpixel level, since multiple land cover types can be detected with a

single pixel. This results in a more realistic representation of the true nature of the area under study.

Most SMAs use linear mixture models, whereby the observed spectral response of a pixel is assumed to be a linear mixture of the individual spectral signatures of the land cover types present within that pixel. These individual or "pure" reference spectral signatures are referred to as endmembers[1], because they represent the cases where 100 percent of the sensor's field of view is occupied by a single cover type (Lillesand & Kiefer, 2000).

The linear mixture model assumes that the weight given for any endmember's signature is the proportion of the area occupied by the class defined by that endmember. The linear mixture model considers the spectral signature of each pixel in the image. Using linear unmixing, it determines the proportion of each endmember present in each individual pixel and creates a fraction image for each endmember.

Lillesand & Kiefer (2000) set out the two basic conditions which have to be satisfied mathematically for linear mixture analysis.
"Firstly, the sum of the fractional proportions of all potential endmembers included in a pixel must equal 1. Expressed mathematically,

$$\sum_{i=1}^{N} Fi = F_1 + F_2 + \ldots + F_N = 1$$

where F_1, F_2, ..., F_N represent the fraction of each of the N possible endmembers contained in a pixel."

The second condition which must be met (Lillesand & Kiefer, 2000) is that "for a given spectral band λ the observed digital number $DN\lambda$ for each pixel represents the sum of the DNs that would be obtained from a pixel that is completely covered by a given

[1] Pure reference spectra or endmembers can be measured using a spectrometer in a laboratory or in the field. They can also be measured using a known "pure" land cover type from the image itself.

endmember weighted by the fraction actually occupied by that end member plus some unknown error. This can be expressed by

$$DN_\lambda = F_1 DN_{\lambda,1} + F_2 DN_{\lambda,2} + \ldots + F_N DN_{\lambda,N} + E_\lambda$$

where DNλ is the composite digital number actually observed in band λ; F_1, …, F_N equal the fractions of the pixel actually occupied by each of the N endmembers; $DN_{\lambda,1}$, …, $DN_{\lambda,N}$

equal the digital numbers that would be observed if a pixel were completely covered by the corresponding endmember; and $E\lambda$ is the error term."

If SMA is carried out on multi-spectral data, the number of versions of equation 2 would equal the number of spectral bands contained in the data. So for X spectral bands, there would be X equations, excluding equation 1. So there would be $X + 1$ equations available to solve the endmember fractions (F_1,…,F_N). Following on from this; if the number of spectral bands exceeds the number of endmembers in an image, then the set of equations including the error term can be solved. However if the number of endmembers exceeds the number of bands, there will not be a unique solution to the equations. It therefore follows that, the more bands contained in an image, the more endmember classes can be identified (Lillesand & Kiefer, 2000).

Where the object of interest is only one land cover type, partial unmixing can be used instead of linear spectral unmixing. This technique uses matched filtering to find the abundance of user-defined endmembers in a scene. Matched filtering has the advantage that not all endmembers in a scene need to be known. The technique maximizes the response of the known endmember and suppresses the response of the composite unknown background, thus "matching" the known signature. Its advantages are;

1. It is a quick method of detecting specific land cover types based on matches to library or endmember spectra; and

2. It does not require knowledge of all the endmembers within an image scene. (Research Systems, Inc, 2001).

Before continuing in the discussion on partial unmixing, it is first necessary to explain the techniques used in the partial unmixing process, namely Minimum Noise Fraction transform (MNF) and the Purest Pixel Index (PPI).

5.2.6. Minimum Noise Fraction Transform

The Minimum Noise Fraction transform (MNF) is a modified version of the Principal Component Analysis that orders the output components by decreasing signal to noise ratio (Microimages, 2001). Principal component analysis is designed to reduce redundancies in data by compressing it into fewer numbers of bands, whereby the majority of the important image information will be contained in the low-order components, while noise increases with increasing component number. If bands in an image have differing amounts of noise, standard principal components derived from them may not show the usual trend of steadily increasing noise with increasing component number.

The MNF procedure estimates the noise in each image band and then applies two successive PCAs. The noise is estimated from the image using the variations in brightness for each pixel compared to the mean (or noise free) image. Two PCAs are then applied. The first PCA uses the noise estimates to transform the dataset to a coordinate system in which the noise is uncorrelated and is equal in each component. This is known as noise whitening. Then a standard principal component analysis is applied to the noise-adjusted data. This methodology results in a set of components in which noise levels increase uniformly with increasing component number. In other words, the low-order components should contain most of the image information (signal) and little image noise (Microimages, 2001)

5.2.7. Pixel Purity Index (PPI)

The PPI is a method used in multi-spectral and hyperspectral image processing which identifies the most "spectrally pure" pixels in an image. These "pure" pixels typically correspond to endmembers (Research Systems, Inc, 2001). In most instances, the PPI is applied to low-order MNF components (Van der Meer, De Jong & Bakker, 2001), as these represent condensed versions of the high importance (signal) data contained in the original image.

When image spectra are plotted as points in n-dimensional space, endmember spectra should be the outliers along the edge of the data cloud. The PPI is computed by repeatedly projecting n-dimensional scatter plots in a random direction. The extreme or outlying pixels in each projection are recorded, and the total number of times each pixel is marked as extreme, is noted. A PPI index is created in which the DN of each pixel corresponds to the number of times that pixel was recorded as extreme (Microimages, 2001). Pixels with high values in the resulting PPI image identify the locations in the data space of the initial set of spectrally pure endmembers (Van der Meer, De Jong & Bakker, 2001).

5.2.8. Matched Filtering

The Matched Filtering algorithm assesses the spectral composition of each pixel. Each pixel spectrum is assumed to be a linear mixture of endmember spectra and multiple unknown spectral signatures. The matched filtering process identifies what proportion (if any) of each individual pixel's spectrum is made up by the endmember spectrum. The mathematics behind this algorithm is complex and will not be discussed. However, interested readers are referred to Jacobsen, Heidebrecht & Nielsen (1998). Simplistically explained by Microimages (2001), a perfect match yields an output value of 1, while poor matches yield low positive or even negative values. An image can then be displayed of the results where linear contrast enhancement can accentuate areas containing a high proportion likelihood of containing the target endmember.

In an example from the literature Jacobsen et al. (1998), successfully used partial unmixing of CASI[1] data to monitor the encroachment of shrubs in grassland areas. They concluded that matched filtering works well when the desired endmembers are the covariance drivers of the image statistics. They found that rare objects must have a significant spectral signature in order to be identified.

[1] CASI: The Compact Airborne Spectrographic Imager is a hyperspectral instrument which collects data in 288 spectral channels at 1.9nm intervals in the spectral range 0.4-1.0μm.

CHAPTER 6

METHODOLOGY

The methodology used in this research is threefold. Firstly the methodology proposed by Thompson et al. (2002), for use with Landsat imagery and mentioned in Chapter 5.1 was adapted and used. Secondly, this methodology was modified for use with Aster imagery and the Aster images were processed. Thirdly, as Aster contains 14 bands (see Appendix B) it can be regarded as a hyperspectral image and hyperspectral processing techniques were applied to it. In this Chapter, the methodology proposed by Thompson et al. (2002) will be discussed (Chapter 6.1) in order to familiarize the reader with this particular method. The choice of data and its preparation for use in this dissertation are detailed (Chapter 6.2), followed by the methodologies used in this dissertation (Chapter 6.3 & 6.4).

6.1. Background to Methodology (Description of Technique used by Thompson et al. (2002)

6.1.1. Data Preparation

The data preparation stage of Thompson et al.'s work involved standardizing all Landsat imagery prior to image classification. This included: atmospheric and radiometric correction, georegistration and ortho-rectification and topographic normalization. Thompson et al. (2002) stated that with the exception of georegistration and ortho-rectification, data preparation was not necessary as the classification was image based and not dependent on field measurements acquired at the time of satellite overpass.

6.1.2. Data classification

The first stage of the processing proposed by Thompson et al. (2002) was to create a land cover map of the study area. This land cover map was used to identify, mask and exclude from further processing those land cover categories where wetlands cannot occur e.g. built-up areas or areas where wetlands are so modified that they will not be able to be distinguished from the land cover class which has modified them e.g. agriculture. This mask was created by a progressive sequence of unsupervised classification (see Chapter 5.2.4.1) which was carried out on a generated dataset. The generated dataset was the first five principal components (see Chapter 5.2.1) of a stacked dataset containing the following: 12 original Landsat bands (six from the dry season image and six from the wet season image) and the NDVI (see Chapter 5.2.3) for the wet season and the NDVI from the dry season image. The first 5 principle components (PC) were used in order to compress the data and decrease computational time required for classification. The classification results were then examined and a mask layer was created of those areas which cannot contain wetlands. This mask was then applied at a later stage to exclude from classification, those areas where wetlands cannot occur.

The next step in the processing as described by Thompson et al. (2002) involved the creation of a multi layered file in the following manner:

The tasseled cap transformation (see Chapter 5.2.2) was applied to the wet season and the dry season image independently and the greenness and wetness indices[1] of each season saved. Using these indices, the NDVI[1] of each season which was created earlier, and the mask band, a multi layered file was created as follows:

1. Tasselled Cap Greenness index of wet season image
2. Tasselled Cap Wetness index of wet season image
3. NDVI of wet season image
4. Tasselled Cap Greenness index of dry season image
5. Tasselled Cap Wetness index of dry season image
6. NDVI of dry season image
7. Mask band

[1] The brightness index is not used as it is only the greenness of the vegetation and the wetness of the soil which is of interest.

The ISODATA method of unsupervised classification was then applied to this file to create a classified image. The output of this classification consisted of either one or more classes which were potentially wetlands. Thompson et al. (2002) found that the degree of confidence could vary from class to class or be uniform.

Thompson et al. (2002) then applied hydrological modelling techniques to a digital elevation model (DEM) of their study area in order to identify areas where wetlands should occur according to the morphology of the landscape. The results of the hydrological modelling were then combined with the results of the image classification to give a final classification of wetlands.

In the pilot project (Thompson et al., 2002) to map wetlands using remote sensing, the Department of Environmental Affairs and Tourism set the following aims: to map 90 percent of all wetlands greater than1 ha and 50 percent of all wetlands less than 0.5 ha. The report by Thompson et al. (2002) concluded that where small wetlands were present, medium resolution satellite imagery was not suitable for wetland mapping. However medium resolution satellite imagery can indicate a general presence or absence of small wetlands but cannot be used for accurate mapping purposes. In addition, they noted that vegetated wetlands generally had a lower mapping accuracy than open-water wetlands.

6.2. Data choice and Preparation for this Dissertation

The best time of year for the satellite images to be acquired is when the wetlands exhibit the most differences spectrally to the surrounding vegetation. This is especially true in the case of vegetated wetlands. This period is usually during the transitional 'wet-up' or 'dry-down' periods. In the summer rainfall areas, within which the study area falls, the optimum wet-period image period is likely to be from September to November. This is just after the onset of the summer rains when the wetlands are inundated and experiencing vigorous early season growth compared with the surrounding non-wetland

[1] The NDVI is used as is a greenness or biomass index and wetland and non-wetland areas should give different responses in a NDVI.

vegetation. By the same reasoning, the optimal dry season image acquisition time is from March to May as wetlands are likely to remain wetter and greener for longer into the dry season than the surrounding non-wetland vegetation. Multi-temporal datasets (one wet-up and one dry-down image) are highly desirable. However where only single date imagery exists, it is possible to utilize this provided the image acquisition period is optimal. (Thompson et al., 2002)

The rainfall of Queenstown was carefully studied (Figure 14), as Queenstown is the closest weather station to Qoqodala with complete rainfall data. Using this data, optimal dates for two Landsat images and an Aster image were selected. The dry season Landsat TM image was selected from May 1984, a wet-season Landsat ETM+ image was selected from November 2000; and as only wet-season Aster imagery was available, October 2000 was selected. These dates fulfil the above criteria laid out by Thompson et al. (2002) for optimal image acquisition dates and all images were cloud free.

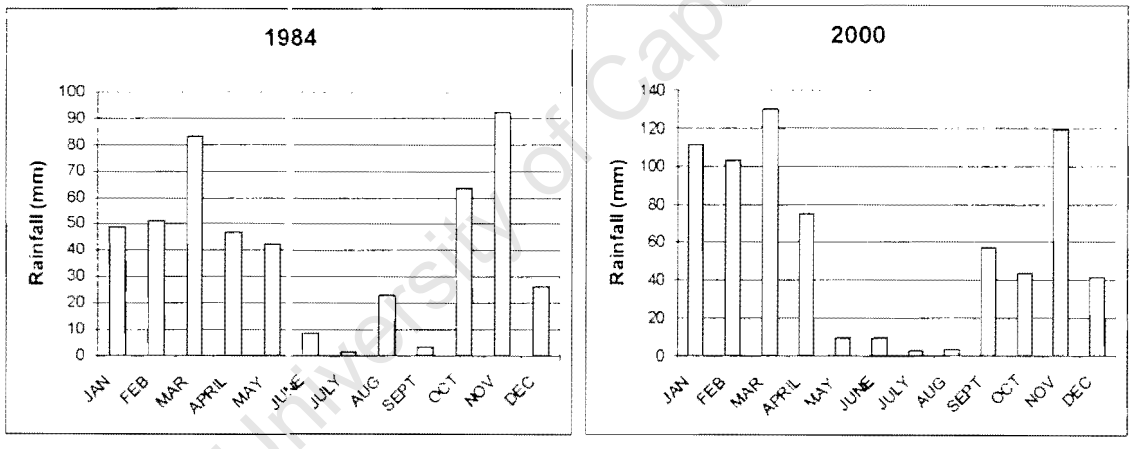

Figure 14: Rainfall data of Queenstown for 1984 and 2000 (Data obtained from S.A. Weather Services)

The Landsat TM image was ordered from the NASA website to a level of processing 1B which means that the image is orientated to a map projection, but it is not ortho-rectified. The Landsat ETM+ image was ordered ortho-rectified from the Satellite Application Centre. Finally the Aster image was ordered from the NASA Aster website also to a processing level of 1B. The Landsat TM and Aster image were then rubber-sheeted to

match the Landsat ETM+ image using ERMapper® Geoprocessing Wizard. Before this process could take place, the Aster short wave infrared (SWIR) bands were resampled to 15metres in order to match the visible and near infrared (VNIR) bands.
Universal Transverse Mercator (UTM) Zone 35 South based on the WGS84 datum was the map projection chosen for the research.

ErMapper® 6.2 was used in the data preparation stages of the research. For all image processing beyond the georeferencing / orthorectification stage, ENVI® 3.5 was used. ArcView® 8.1 was used for all vector data processing, spatial analysis and map production, and the extension ArcView® Spatial Analyst was used when required.

A base map was prepared using data gathered during the initial field trip; then during subsequent field trips, the base map was expanded. This base map was used to assess the validity of results obtained in the office before field verification was undertaken. This base map can be seen in Figure 15.

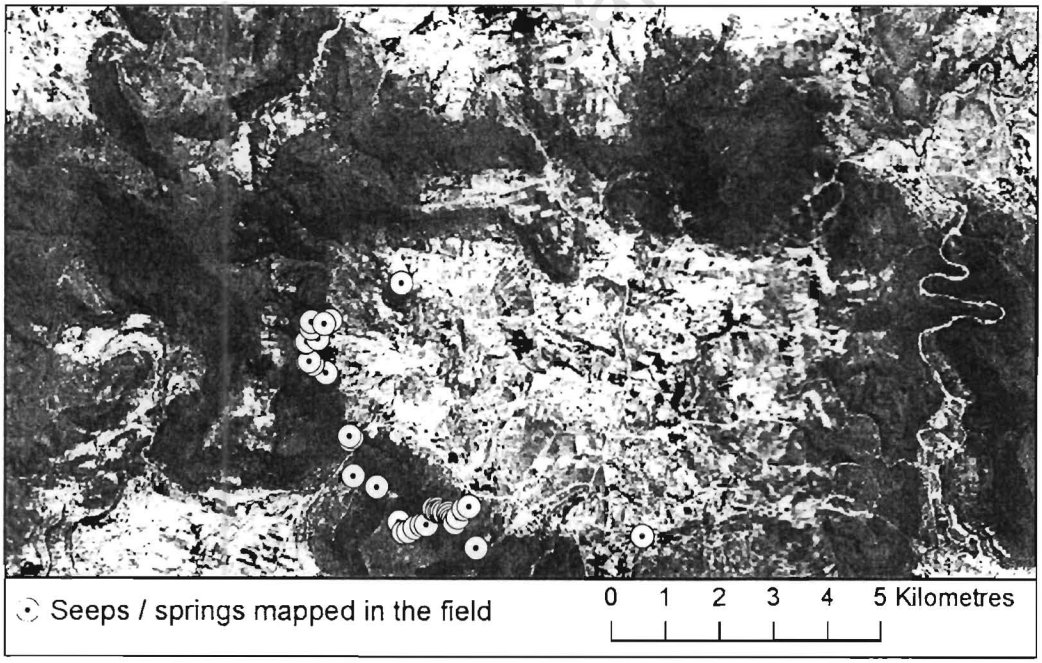

Figure 15: Base map

6.3. The Landsat Classification Approach

This methodology is based largely on the proposal by Thompson et al. (2002) with two major exceptions. Firstly, the process of creating a land cover map to exclude areas which cannot contain wetlands was modified. Secondly, the final hydrological modelling stage was also excluded from the research. After carrying out the image processing it was apparent that the hydrological modeling stage would not add any further values to the results. A flow chart depicting the various steps in this approach can be seen in Figure 16.

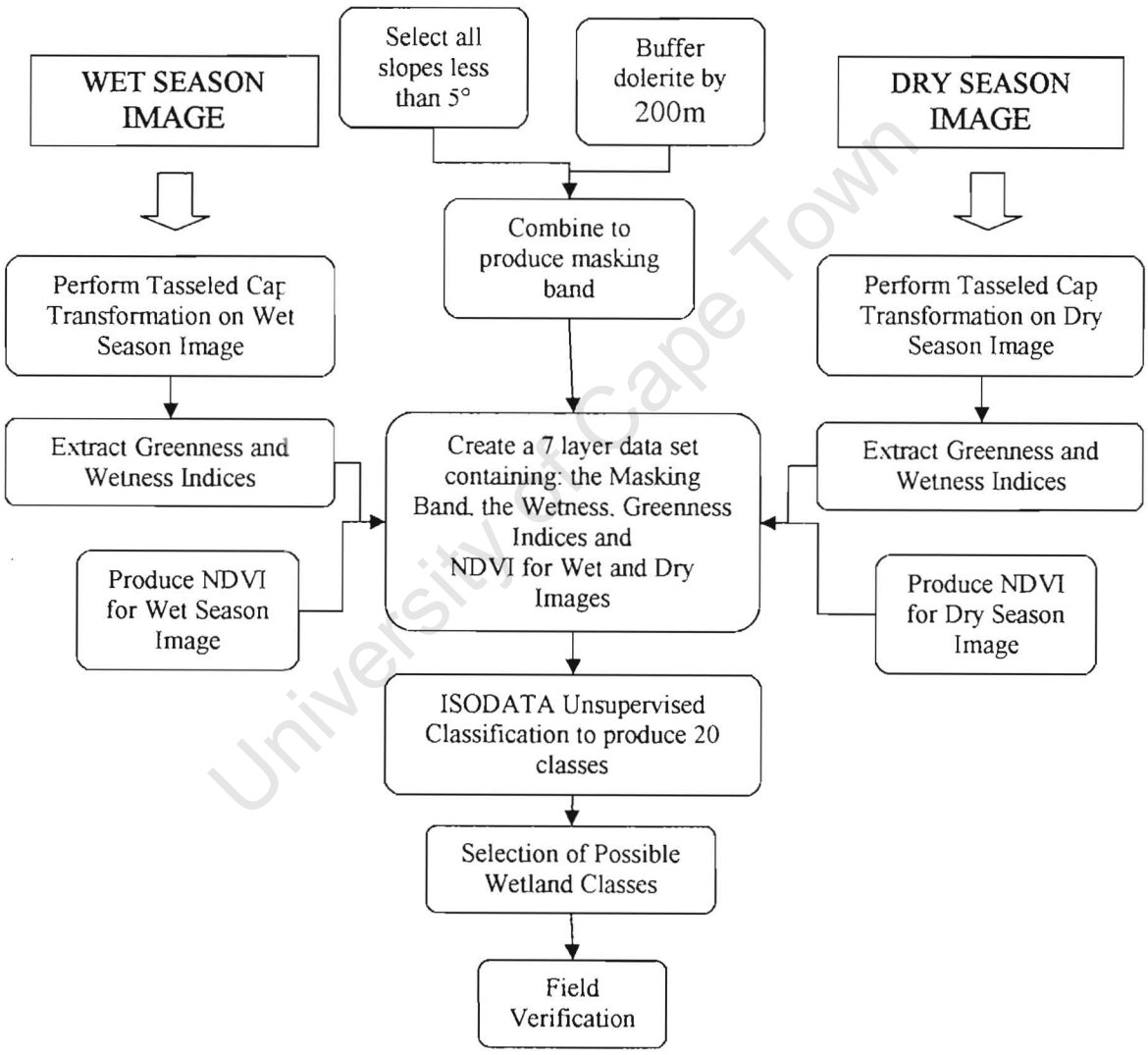

Figure 16: Flow Chart of methodology used in the Landsat Classification Approach

Instead of creating an initial land cover map, it was decided to rather exclude the flat inner ring from processing. The reason for doing this is threefold. Firstly the seeps tend to occur either on the dolerite or on the contact between the dolerite and the sediment. For the most part, the dolerite forms the slopes of the ring and sediment occurs on the flat inner ring. Secondly, due to the fact that the people rely on rainfall for irrigation, it is highly likely that if wetlands existed in the inner ring in the past, they made an ideal location for crop or pasture and have been changed beyond recognition. Finally, the more homogeneous an image, the better the classification results will be (Smith, Wickham, Stehman and Yang, 2002), so it was decided to exclude the heterogeneous portions of the image which is the flat inner ring and only work with the more homogeneous dolerite upland portion of the image. The heterogeneous nature of the inner ring due to haphazard land use can be seen in Figure 17.

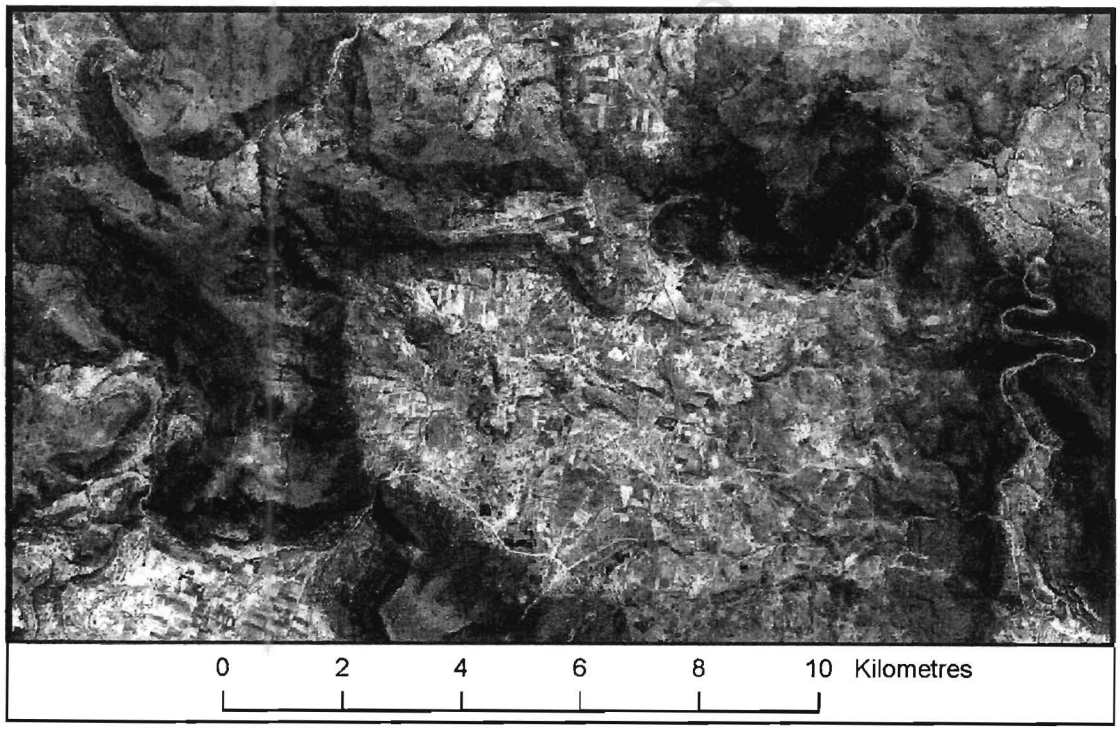

Figure 17: Aster 321 image of Qoqodala

Following on from the above reasoning, a mask was created in the following manner:

1. An ArcView® shape file of the dolerite had been digitized at a scale of 1:50000 for the WRC project. The dolerite was then buffered by 200m to include areas of sediment immediately adjacent to the dolerite, as seen in Figure 18A. This was done in order to accommodate the fact that seeps often occur at the contact between two different geological units.

2. The inner ring does not always consist entirely of sediment. In some cases, the sediment has been eroded leaving the dolerite of the lower sill exposed. This is the case in the Qoqodala ring. However, it was still felt necessary to exclude the inner ring in order to exclude the highly heterogeneous portions of the image. A slope analysis was performed using a digital elevation model (DEM) and all areas with a slope of less than 5 degrees were clipped from the buffered dolerite layer, as seen in Figure 18B. The areas to be included in processing were given a code of 1 and those areas to be excluded a code of 0. The vector layer was then converted to a raster layer and this was used as the masking band (Figure 18C).

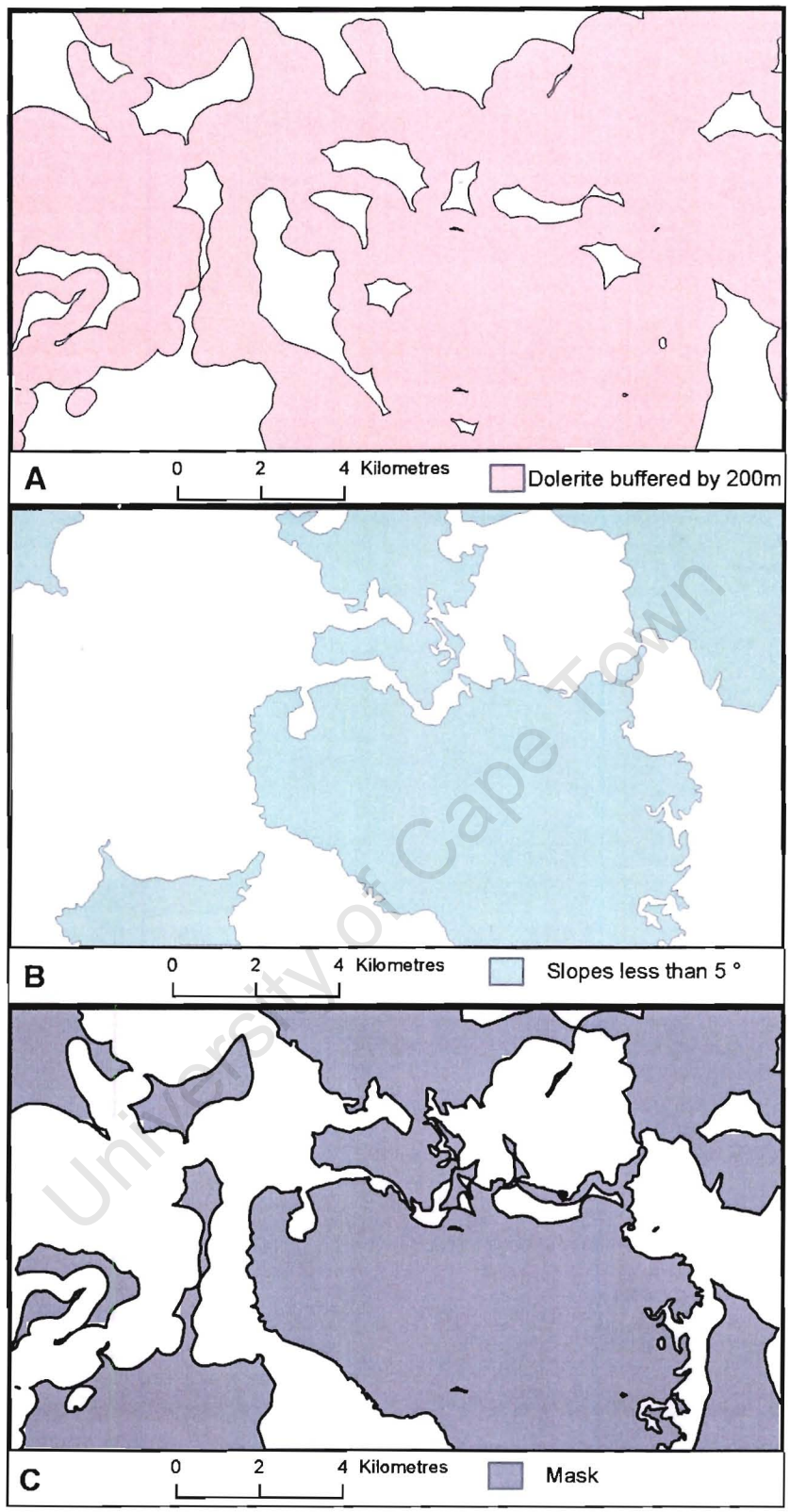

Figure 18: **The mask creation process.** **A: The dolerite is buffered by 200m; B: all slopes less than 5° are isolated and C: A and B are combined to produce a mask**

A tasseled cap transformation was performed on each of the Landsat images, using the above mentioned mask to exclude the inner ring. Similarly a NDVI for each image was produced. These six resulting files were then stacked to create a multi-layered file on which the classification was to be performed.

As per the recommendations by Thompson et al. (2002), an unsupervised method of classification was chosen for this research for the following reasons:

1. Although parts of the study area were very well known, there were some regions such as the mountainous regions which had not been visited. One of the advantages of the unsupervised classification method is that extensive prior knowledge of the region is not required (Campbell, 1996)
2. From the outset it was surmised that the wetlands in question were very small (seeps) and finding training data would be difficult. Small classes which would otherwise be overlooked in supervised classification as they would be included in other larger classes, are maintained when running an unsupervised classification (Campbell, 1996)
3. The aim of the study was not to produce a land cover map but rather to identify one specific land cover i.e. wetlands.

An ISODATA classification was run using ENVI software with a maximum output of 20 classes. The parameters used in the ISODATA classification can be found in Appendix D.

6.4. Methodology used to process Aster Imagery

6.4.1. The Aster Classification Approach

The method proposed by Thompson et al. (2002) was then modified further for use with the Aster image available for the study area. A flowchart of the methodology is given in Figure 19.

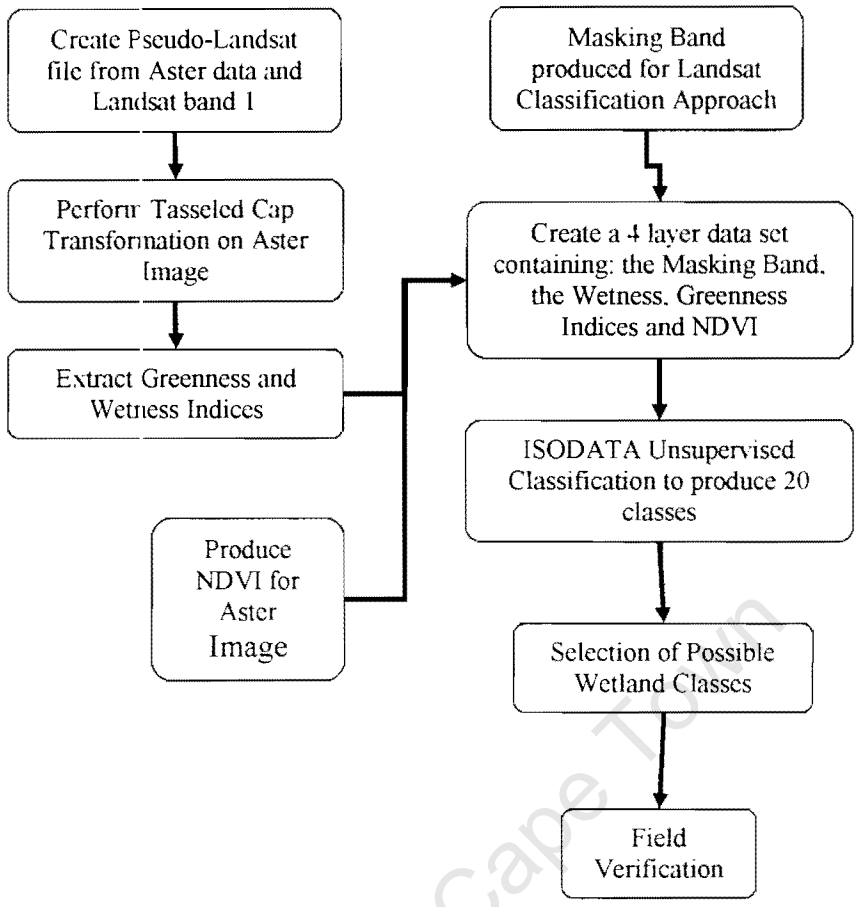

Figure 19: Flowchart of Methodology for Aster Classification Approach

As can be seen in Appendix B, Aster has three bands with a fifteen metre resolution making it a better option for detecting smaller wetlands. However, there are two drawbacks with using Aster in this study. Firstly, only a single date image was available for the study area and, secondly, the wavelengths represented by Aster bands do not correspond exactly with the wavelengths represented by Landsat bands (see Appendix B). This necessitated the further modification of the technique proposed by Thompson et al. (2002).

Ideally, the methodology requires multi-date imagery for this processing, but where only one image is available, a single date image can suffice provided that the image was acquired at an optimal time of year. For vegetated wetland detection, the optimal time of year would be at the onset of the rainy season, as it is at this time that the vegetation in

the wetland will show the most difference compared with the surrounding non-wetland vegetation. Wetlands are first to be inundated with water after the first rains, so wetland vegetation responds earlier in the season than non-wetland vegetation (Thompson et al., 2002). An Aster image was available for 16 October 2000 and as the summer rains began in September that year, this date is considered ideal if using single date imagery. This resulted in the dataset built for classification consisting of only three layers excluding the mask layer: the NDVI for the wet season and the greenness and wetness indices (from the tasseled cap transformation) for the wet season. This is in contrast to the six layers, excluding the mask layer used in the Landsat classification approach.

The differences in band wavelengths between Aster and Landsat presented a particular challenge. The methodology required the application of the tasseled cap transformation (TCT) to the data. This is problematic as the TCT was developed for Landsat imagery and not Aster imagery. A concern of the author was whether the application of a technique specially developed for Landsat image on Aster image is scientifically valid. Personal correspondence with Prof. Paul Mather suggested a method whereby coefficients of the tasseled cap transformation could be calculated specifically for Aster image data. This method is dependent upon the definition of the soil line and involves the identification of pixels of bare wet soil and bare dry soil. Since it is crucial that these pixels are recorded at the time of the satellite passing overhead, it was not possible to attempt this method. The reader can consult Mather (1999) for further reading on this subject. Since it was not possible to calculate coefficients for Aster imagery and the results were to be used qualitatively and not quantitatively, it was decided to use the standard coefficients and assess the results.

There is no equivalent for Landsat band 1 in the Aster bands and conversely there are four Aster bands that fall in the range of Landsat band 7. There appeared to be no alternative but to simply use Landsat band 1 resampled to 15m for the TCT on the Aster data. The ratio of input of each band to output index (see Table 1 below) was examined and it was discovered that band 1 most influences the output of the dryness and to a lesser

extent the greenness index. Band 1 also has minimal influence on the wetness output index. It was thus decided that this was an acceptable solution.

Table 1: Coefficients for the tasseled cap functions 'brightness', 'greenness', and 'wetness' for Landsat Thematic Mapper bands (Mather, 1999)

TM Band	1	2	3	4	5	7
Brightness	0.3037	0.2793	0.4343	0.5585	0.5082	0.1863
Greenness	-0.2848	-0.2435	-0.5436	0.7243	0.0840	-0.1800
Wetness	0.1509	0.1793	0.3299	0.3406	-0.7112	-0.4572

Landsat band 7 covers the wavelengths represented by Aster bands 5, 6, 7 & 8. Correlation statistics were carried out in order to determine which of these bands correlated best to Landsat band 7. Additionally, the mean of the five bands was calculated, as was the first principal component and correlations between these two outputs and Landsat band 7 were also examined. The results, shown in Table 2 below, indicated that all the outputs were similarly correlated, with Aster band 7 slightly outperforming the rest

Table 2: Correlations between Landsat band 7 and Aster bands.

	Landsat Band 7	Aster Band 5	Aster Band 6	Aster Band 7	Aster Band 8	Mean Aster 5-8	1st PC Aster 5-8
Landsat Band 7	1	0.771876	0.761988	0.772333	0.767489	0.772188	0.772201

A pseudo-Landsat file was thus built as follows:

Band 1 = Landsat band 1

Band 2 = Aster band 1

Band 3 = Aster band 2

Band 4 = Aster band 3

Band 5 = Aster band 4

Band 7 = Aster band 7

Band 6 was excluded as it is the thermal infrared band and these bands were not used due to their coarse resolution.

The tasseled cap transformation was then run on this file using ENVI® software and the Greenness and Wetness Index was extracted and saved for later processing.

The NDVI utilizes the near infrared and the visible red bands in its calculations. It is not sensor dependent and can be used with any sensor's data containing these wavelengths. In the Aster bands, band 3 is the near infrared band and band 2 is the visible red band and as such, these were the two bands used in the calculation of the NDVI.

A multi-layer dataset was then created using the NDVI and the Greenness and Wetness Indices from the TCT. An ISODATA unsupervised classification was run on this dataset in the same way and using the identical parameters as in the case of Landsat.

6.4.2. Processing Aster as a Hyperspectral Image

Instead of simply modifying and applying an already developed methodology, it was decided to test an alternative method. In order to expand the research, it was decided to regard the Aster image as a hyperspectral image and apply hyperspectral processing techniques to the image. Figure 20 details the methodology used in processing the Aster Image as a hyperspectral image.

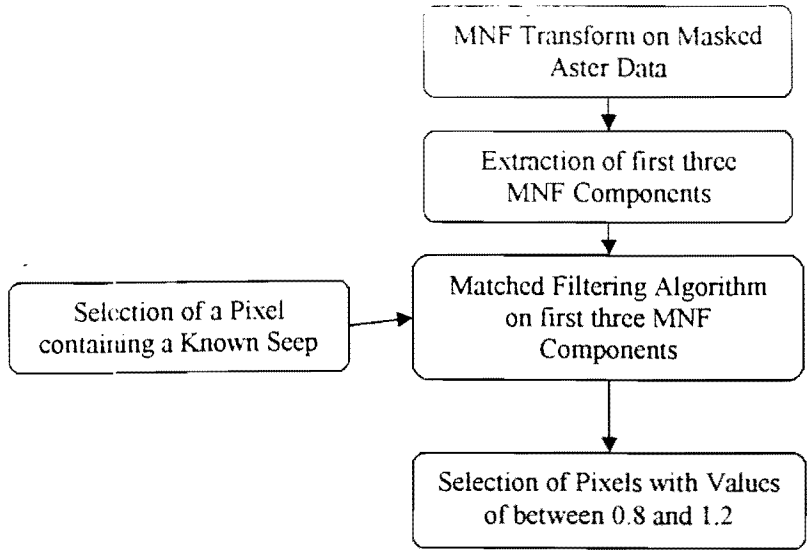

Figure 20: Flowchart of the methodology used in the hyperspectral processing of the Aster image

As has been seen from the field work conducted, the wetlands which are being attempted to map are in many cases smaller than the pixel size of the images. "The extent to which mixed pixels are contained in an image is a function of the spatial resolution of the remote sensing system used to acquire the image and the spatial scale of the surface features in question" (Lillesand & Kiefer, 2000). In other words, what is occurring is a mixed pixel effect in that there are more than one land cover types captured within the sensors instantaneous field of view. The features that are being mapped are occurring at a sub-pixel level. Spectral mixture analysis is a procedure which is designed to classify mixed pixels and is a way to accomplish sub-pixel classification (see Chapter 5.2.5.).

Given the above, it would be prudent to use the Aster image for spectral mixture analysis rather than Landsat, as Aster contains more bands and the equation could be solved for more endmembers. However, in this study it is not necessary to identify all possible endmembers in a scene for the reason that only seeps/wetlands are being mapped.

In this study this may present difficulties, as the wetlands which are being assessed consist primarily of grass and thus may be spectrally very similar to grasslands. It is unlikely that the wetlands in this case have a significant spectral signature. According to Gorte (In Stein et al. 2002), in order to obtain information from multi-spectral imagery, the multi-dimensional continuous reflection measurements have to be transformed into discrete objects which are distinguished from each other by a discrete thematic

classification. However, within different objects of the same class and even within a single object, the reflection is not always the same. Conversely, different thematic classes cannot always be distinguished in a satellite image because they display almost the same reflection. In cases such as these, deterministic methods such as unsupervised classification will not be successful and an alternative method should be found. It is hoped that matched filtering will be that successful alternative method. Please note that explanations of the techniques about to be discussed can be found in Chapter 5.

Spectral mixture analysis can only create a maximum of n + 1 endmembers in a scene where n = the number of bands in the image. The Aster dataset contains nine bands[1] so a maximum of ten endmembers can be identified. Upon running the spectral mixture analysis, the known seeps were not isolated as being endmembers so an alternative method had to be found. It was decided to use matched filtering (also known as partial unmixing). The matched filtering process requires the identification of endmembers in the scene. These can be identified by running the PPI on a low order MNF component. Alternatively, if the land cover of interest is not identified as an end member after running the PPI, a user defined endmember can be used. In this case, pixels of interest are selected by the user and defined as endmembers. The partial unmixing process can then run using the user defined input endmembers in place of the PPI identified endmembers.

[1] The thermal bands were not used in the processing due to their coarse resolution.

CHAPTER 7

RESULTS

7.1. Results of Landsat Classification Approach

The classification image that was produced did not indicate any one class representing the known seeps so it was presumed that these wetlands were too small to be detected (see discussion of results in Chapter 8). It is possible that perhaps larger wetlands were present higher up the slopes in areas that had not been visited in the field and visual interpretation of the image revealed the probable occurrence of grasslands. Since the seeps lower down the slopes are characterized by grass, it was presumed that the grass on the higher slopes could potentially contain wetlands. In addition, dense vegetation growing in river valleys could be identified by visual inspection of the unprocessed image. As these valleys and kloofs are potentially moister areas, these areas are also of interest to the study. With the above in mind, five classes which could potentially contain wetlands were selected with three 'types' of potential wetlands being identified.

The first type consisted of one class and was provisionally called kloof vegetation. It was believed that this class constituted vegetation growing in kloofs, high shadow and moist areas or along riverbanks. Two further types were identified and provisionally called wetlands type one (made up of one class) and wetlands type two (made up of two classes). Wetlands types one and two were mostly located on the highest parts of the slope in areas that probably received the most precipitation and as a result, the potential for finding wetlands is greater. Fieldwork would later reveal the characteristics of wetlands type one and two. The three types of wetland classes were then vectorised. Area calculations revealed the following: Kloof vegetation: 2130217m^2. Wetland type one: 8909743 m^2. Wetland type two: 12699987 m^2 (Figure 21).

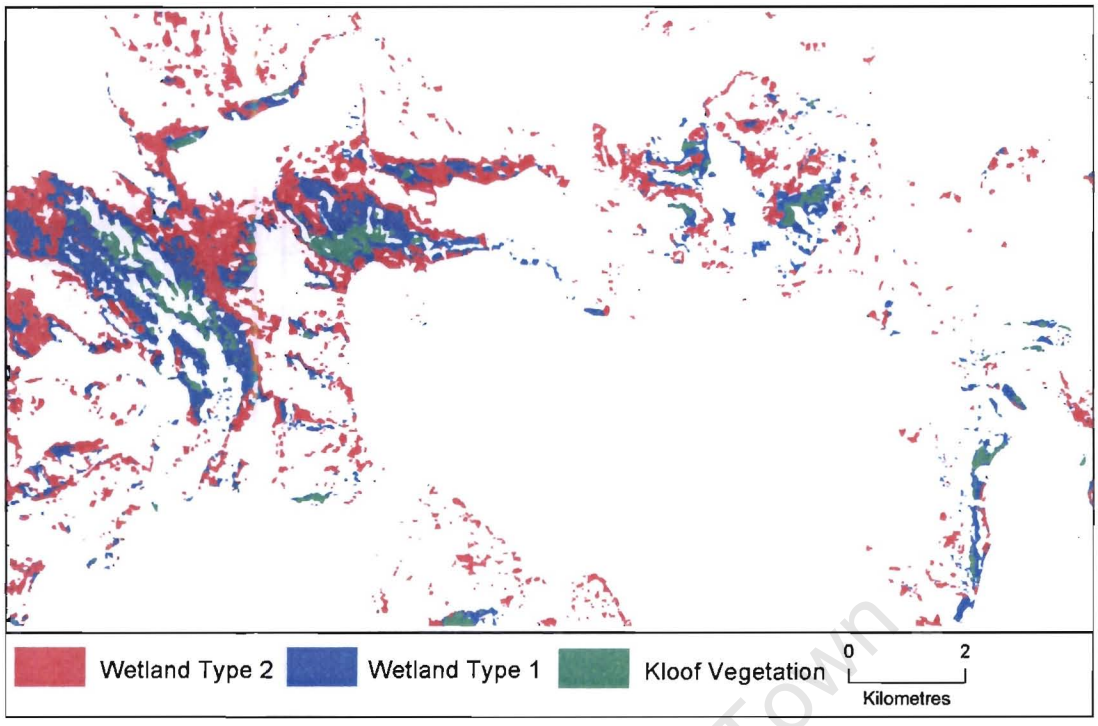

Figure 21: Results of the Landsat Classification Approach

7.2. Aster Imagery

7.2.1. Results of Aster Classification Results

Similarly to the results of the Landsat classification approach, the results of the processing on the Aster imagery produced 20 classes with no one class representing the known seeps. The three wetland types, identified using the Landsat classification approach, were matched to the results from the Aster classification. Kloof vegetation in the Aster image was made up of three classes and covered a larger area: 4474125 m^2. Wetlands type one consisted of one class and covered an area of 7343837m^2. Wetlands type two is made up of two classes and the area covered was 12699987 m^2. These results can be seen in Figure 22.

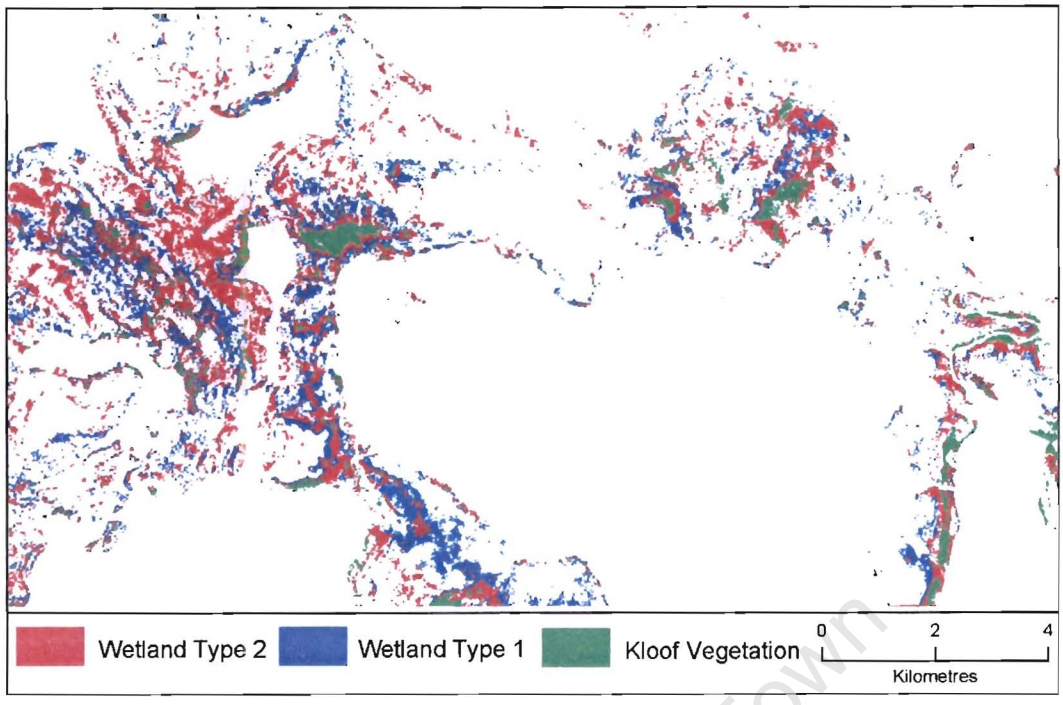

Figure 22: Results of the Aster Classification Approach

It is apparent was that the Aster imagery tends to select smaller areas for each class than Landsat but the difference between total area covered (with the exception of kloofs) does not appear to be significant. A comparison between the results obtained using the Landsat classification approach and the Aster classification approach is given in Table 3.

Table 3: Total area covered by each wetland type.

	Total Area (m2)	Mean Area m2)	No polygons	No classes
Aster: Kloof	4474125	2048	2184	3
Aster: Type 1	7343837	1380	5319	1
Aster: Type 2	9014726	1550	5813	2
Landsat: Kloof	2130217	8486	251	1
Landsat: Type 1	8909743	9027	987	1
Landsat: Type 2	12699987	8627	1472	2
Total Aster (excluding kloof) = 16358563m^2				
Total Landsat (excluding kloofs) = 21609730m^2				

7.2.2. Results of Hyperspectral Processing Techniques

The matched filter algorithm was run on the first three minimum noise fraction components (see Chapter 5). The matched filter algorithm produces a greyscale image with values around 1. A value of 1 indicates an exact match to the input pixel and the further from 1 the value moves, the less of a match the pixel is to the input pixel. The result of this matched filter algorithm produced values which range from -4 to +4. Values of between 0.8 and 1.2 are considered to be close to one and these values were used to create the map of the results (Figure 23).

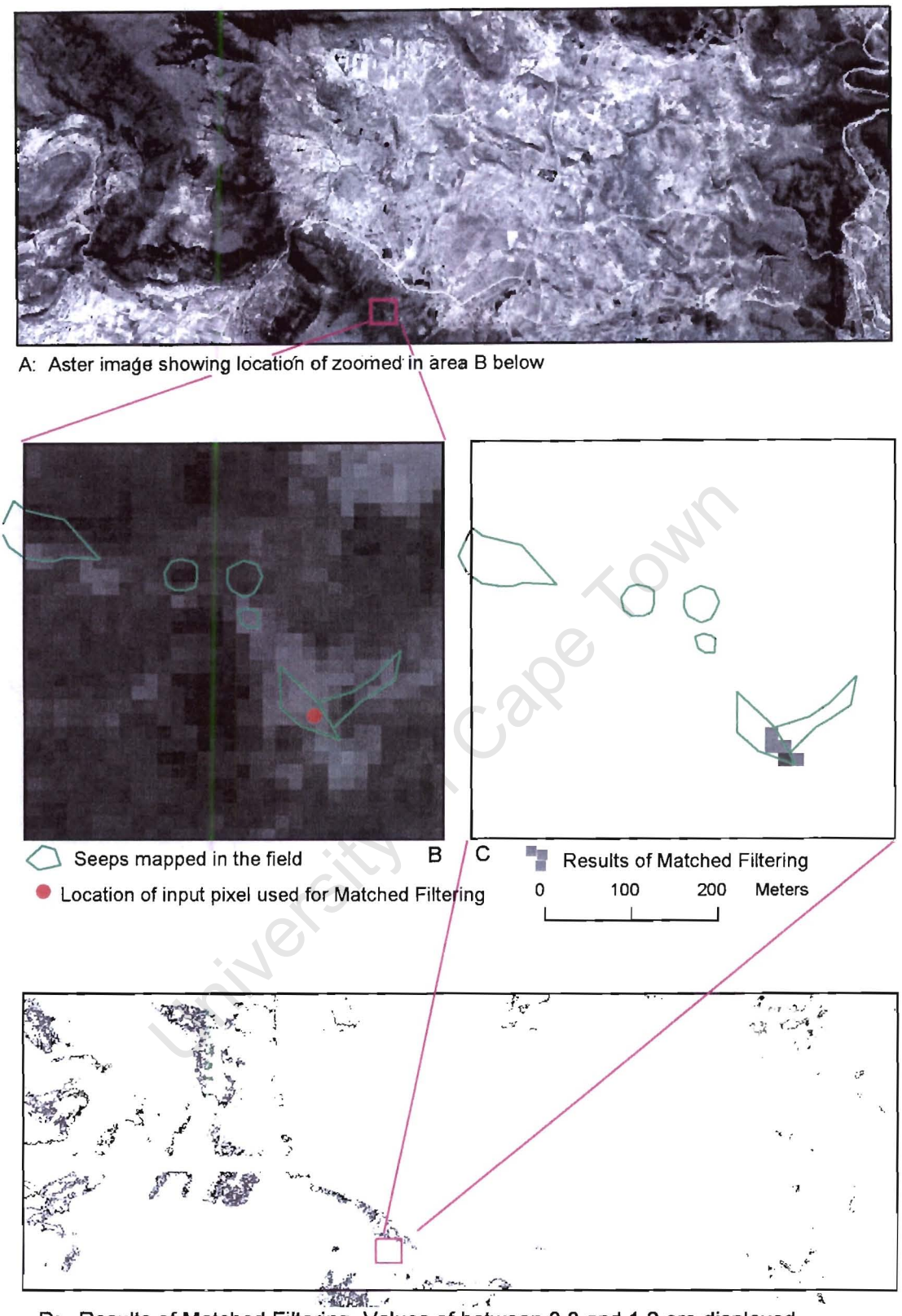

Figure 23: Results of the Matched Filtering Approach

7.3. Field Verification of Results

Fieldwork was carried out in March 2003. The study area was divided into four areas that covered the largest areas of suspected wetlands (Figure 23). The aim was twofold. Firstly to visit the four areas and do a "presence or absence" check to determine whether or not the classes selected are in fact wetlands. Secondly if there are wetlands present, one area would be chosen and the accuracy of the results of the Landsat classification approach to the results of the Aster classification approach would be compared.

After a field trip to all four areas, it became apparent that what had been identified as being a wetland type 1 and wetland type 2 was in fact grassland which was being used as pasture for cattle. There was no visible difference between 'wetland' type 1 and type 2 except that perhaps type 2 was more of a mixed type of grass and small loose boulders or interspersed with small shrubs, whereas type one tended to consist mostly of grass.

The following could explain why the Aster classification approach did not detect as many 'wetlands' as the Landsat classification approach:

The Aster image was acquired in October 2000 and the Landsat image was taken in November 2000. The summer rain of 2000 began in September which means that the landscape captured by the Landsat image was exposed to a month more rain than the landscape captured by the Aster image. In that month the temperature would have increased, the daylight hours would have extended and these coupled to the additional rainfall would have induced grass growth. So the landscape captured in the Aster image simply does not have as much green grass as the landscape captured by the Landsat image.

From this result, it was unnecessary to conduct a more detailed survey of one of the four areas as there were no wetlands to be surveyed. It was also not practical to try to determine the respective accuracy of the Landsat classification approach and the Aster classification approach in terms of pasture mapping, as the season in which the fieldwork

was being conducted (March) differed to the time of year of image acquisition (October and November).

Figure 24: Areas selected for checking presence or absence of wetlands

CHAPTER 8

DISCUSSION OF RESULTS

It can be seen by the results presented in the previous chapter that the methodology selected for this research was not successful in the study area. In this chapter possible reasons for this will be discussed.

The first problem encountered which became apparent after field work at the start of this research was the size of the wetlands in the study area. After initial processing it became obvious that the small seeps which had been located on the side of the slopes during field work were not being detected using the methodology of the project. At that point it was decided to see if these small seeps were the only wetlands present in the study area or if there were in fact larger wetlands perhaps on the upper slopes that had not been discovered during initial field work. The classes that were selected as possible wetland classes were found to be pasture/ grasslands on field checking.

In order to try to understand why the methodology was unsuccessful, the following issues need to be addressed:

1) Size of the individual entity which was attempted to map
2) Scene characteristics

For this discussion Curran and Atkinson (1999) and Smith et al. (2002) were referred to frequently. Curran and Atkinson (1999) address the issues of scale and the choice of an optimum spatial resolution (pixel size) for the study of our environment using remotely sensed data.

"An observer trying to estimate the length of England's coastline from a satellite will make a smaller guess than an observer trying to walk its coves and beaches, who will make a smaller guess in turn than a snail negotiating every pebble" (Mondelbrot, In Curran & Atkinson, 1999).

This observation illustrates that the length of a phenomenon depends on the spatial resolution at which it is measured. According to Curran and Atkinson (1999) the similar conclusion that remotely sensed observation of a phenomenon depends on its area (i.e. its pixel size) is rarely drawn.

Curran and Atkinson (1999) illustrate using an example:
"...imagine measuring the perimeter of your hand with a 1cm long ruler and a 1mm long ruler. The 1mm long ruler would capture more of your hands variability and the perimeter would be longer than if the 1cm long ruler had been used. Likewise, if we asked you to estimate the brightness of your hand over 1 cm x 1 cm squares and 1 mm x 1mm squares then although the average brightness would be the same, the variability would have a larger range. The hundred 1 mm x 1 mm squares within each 1 cm x 1 cm square would not all possess the same value of brightness and in capturing more of your hands variability, would have a larger range. In other words, the variability in brightness of a surface is dependent upon pixel size and it follows that the degree of this dependency is related to the spatial properties of that surface."

An example of this in remote sensing would be in agricultural regions where the dominant spatial frequency of the scene is determined by the dimensions of a typical field. In this case, the land cover will be most accurately mapped if field sized pixels are used. If pixels smaller than a field are used, then the within field observations will be observed and cause misclassification. Similarly, if pixels larger than a field are used, then classification accuracy decreases as interference between fields occurs. (Curran & Atkinson, 1999)

When using Landsat and Aster imagery, the size and the shape of the pixels are constant. As a consequence of these constants, geostatistic techniques that make use of this spatial autocorrelation can be used to understand the influence of pixel size on remotely sensed observations and the environment they represent. Curran and Atkinson (1999) can be referred to for the mathematics behind the geostatistic techniques.

In the late 80's a series of papers was published that discussed images in terms of spatial autocorrelation between pixels. For example, homogeneous areas were seen as having high spatial autocorrelation (neighbouring pixels were similar) such that a coarse spatial resolution (i.e. large pixel size) would be appropriate, whereas heterogeneous areas were seen as having low spatial autocorrelation (neighbouring pixels dissimilar) so a fine spatial resolution (i.e. small pixel size) would be needed. (Curran and Atkinson, 1999)

Smith et al. (2002) conducted a study to evaluate the impact of patch size and scene heterogeneity on accuracy of classification in land cover mapping. According to Smith et al. (2002), landscape characteristics that have been hypothesized to contribute to pixel misclassification include high land cover heterogeneity, small patch size and convoluted shapes all of which result in pixels being harder to classify. In addition, errors along land cover boundaries may be compounded because a substantial proportion of the signal, apparently coming from a land area represented by a specific pixel, actually comes from that pixel's neighbours (Townshend et al., 2000). This results in a tendency for misclassified pixels to form chains along the boundaries of homogeneous patches.

They concluded that as heterogeneity increases, the probability of misclassifying pixels increases, while as patch size increases, the probability decreases.

The result of applying the pixel purity index to the Aster image was to confirm that the spectral signature of the seeps present in the images is not significantly different to the surrounding signatures as the seeps were not identified as endmembers. The fact that the seeps are not spectrally unique contributes to the lack of accuracy in classification.

CHAPTER 9

CONCLUSION

The objective of the research to establish the possibilities of mapping wetlands in Qoqodala using Landsat and/or Aster Imagery was met. It was discovered that, in the study area, it is not possible to map small wetlands using either Landsat or Aster Imagery.

The methodology proposed by Thompson et al. (2002) and adapted and applied to the study area was unsuccessful in detecting seeps in Qoqodala. This supports the claim by Thompson et al. (2002) that the technique is inadequate for accurate small wetland mapping. However, contrary to the finding of Thompson et al. (2002), in this study area, satellite-based mapping using Landsat-type imagery could not be used to indicate a general presence or absence of wetlands.

The method proposed by Thompson et al. (2002) which was modified for use with Aster imagery was also unsuccessful in detecting seeps in the study area. The higher resolution of the Aster image and the increased number of spectral bands did not make any significant difference to the mapping of seeps in the study area.

Finally, treating Aster as a hyperspectral image and processing it as such did not yield any better results. It had been postulated that hyperspectral processing may have been more appropriate than other classification methods for mapping a single land cover type i.e. seeps. In this study area, this was not found to be the case.

The smaller the patch size of individual land covers, the more heterogeneous the landscape and the less accurate the classification result. Although the most heterogeneous inner ring was masked from the image classification, the landscape was nonetheless too heterogeneous with the patch size of the wetlands too small to be detected using this

imagery and this method. The reason for the lack of success of the methodologies is detailed in the discussion of the results (Chapter 8).

Summarized, the wetlands are too small and spectrally too similar to surrounding vegetation to be accurately mapped using Landsat and Aster imagery. In addition, the landscape itself is very heterogeneous which compounds the difficulties in accurately classifying seeps and wetlands.

CHAPTER 10

RECOMMENDATIONS

The fact that the methodologies used in this research project were unsuccessful in the study area implies that there should be many recommendations.

It is recommended that in order to map seeps in the study area, two methodologies should be considered; near infrared (NIR) aerial photography or field mapping.

NIR aerial photography is very expensive as the photography is not readily available for the study area and would have to be flown. In addition, the exercise of orthorectifying the photographs would have to be undertaken followed by the actual identification and delineation of the wetlands. The costs involved in this process would not be justifiable.

Although field mapping is usually a time-consuming and expensive option, in this particular study area it may be a viable alternative. It was mentioned in the description of the study area in Chapter 3.4 that the majority of the local population is unemployed. The opportunity to empower the community by teaching basic map skills and employing them to do the field mapping could be beneficial to all involved. Quality checks would ensure that accurate mapping was being conducted. However the disadvantage is that once the project is completed, the jobs disappear and in all likelihood, the relief from poverty would only have been temporary.

With regard to the remote sensing result in this research three main reasons for the disappointing results were identified:

- Size of the seeps
- Heterogeneous landscape
- Seeps are not spectrally unique

If the study area and the object to be mapped are well known to the researcher before commencing with the project, the researcher should be able to decide whether or not remote sensing is the right approach for his or her particular study. One of the most important factors to be considered in this decision is the size of the object to be mapped in relation to the scale of the imagery. This should be assessed prior to the purchase of the imagery. Secondly, the homogeneity of the landscape should be evaluated as the more homogeneous a landscape, the more accurate the results of a classification. This decision is often very difficult prior to purchase of the imagery as a landscape may appear uniform to the human eye viewed from a horizontal plane, but appears heterogeneous when viewed from above in a satellite image. Finally, if the spectral response of the object being mapped is very similar to another object in the image, it can be very difficult, if not impossible to distinguish the two. Unfortunately this cannot be determined until the image statistics have been examined and at this point the imagery has already been purchased so the researcher is committed to using that imagery.

The final recommendation is to consider the qualifications of the researcher carrying out the processing of the satellite images. The researcher should be qualified in the science required by the aims of the project e.g. ecologist, geologist, geographer as well as in advanced image processing techniques. Alternatively, researchers should work in multi-disciplinary teams in order to have the necessary expertise in both the natural sciences as well as the statistics and computer knowledge required for advanced image processing.

REFERENCE LIST

Arbuckle, C. J., Huryn, A. D. & Israel, S. A. 1998. Applications of Remote Sensing and GIS to Wetland Inventory: upland bogs. Paper presented at the 10th Colloquium of the Spatial Information Research Centre, University of Otago, New Zealand.

Asmal. K. Parliamentary Media Briefing. Ministry of Water Affairs and Forestry. 16 February 1999. [Online]. http://www.gov.za/speeches/briefings99/water.html [20.6.2003].

Bates, J. A. & Jackson, J. A. 1980. Glossary of Geology. *2nd ed.* Viginia: American Geological Institute.

California Institute of Technology. Aster Instrument Characteristics. [Online]. Http://Asterweb.jpl.nasa.gov/instrument/character.htm. [15.2.2002].

Campbell, J.B. 1996. Introduction to Remote Sensing. 2nd ed. London: Taylor & Francis.

Castano, S., et al. 2000. Wetland monitoring by the integration of remotely sensed data in a GIS. In Casanova, J L. (ed.). *Remote Sensing in the 21st Century: Economical and Environmental Applications,* pp31-36. Rotterdam: A.A. Balkema.

Chevallier, L., Goedhart, M & Woodford, A. 2001. *The influence of dolerite sill and ring complexes on the occurrence of groundwater in Karoo fractured aquifers: a morpho-tectonic approach. WRC Report no 937.* Pretoria: Water Research Commission.

Chevallier, L & Woodford, A. 1999. Morpho-tectonics and mechanisms of emplacement of the dolerite rings and sills of the Western Karoo, South Africa. South African Jouranl of Geology. 102:43-54.

Conrad, J., Hughes, S and van der Voort, I. 2000. The new National Water Act: a case study on the applicability of commercial multi -spectral data for determining the groundwater reserve. 28th International Symposium on Remote Sensing of Environment, Cape Town. Proceedings on CD ROM.

Crist, E. P. & Cicone, R. C. 1984. Application of the Tasseled Cap concept to simulated Thematic Mapper data. *Photogrammetric Engineering and Remote Sensing.* 50:343-352.

Curran, P. J. & Atkinson, P. M. 1999. In Stein, A., van der Meer, F. & Gorte, B. (eds) *Spatial Statistics for Remote Sensing*, pp 115-133. Dordrecht: Kluwer Academic Publishers

Dupigny-Giroux, L. & Lewis, J.E. 1999. A Moisture Index for Surface Characterization over a Semi-arid Area. *Photogrammetric Engineering & Remote Sensing.* 65:937-945.

Frazier, P.S. & Page, K. J. 2000. Water Body Detection and Delineation with Landsat TM Data. *Photogrammetric Engineering & Remote Sensing.* 66:1461-1467.

Jacobsen, A., Heidebrecht, K. B. & Nielsen, A. A. 1998. *Monitoring Grasslands using Convex Geometry and Partial Unmixing – A Case Study.* 1st EARSel Workshop on Imaging Spectroscopy, University of Zurich, Switzerland. Proceedings edited by: M. Shaepman, D. Schlafer & K. Itten.

Lillesand, T. M. & Kiefer, R. W. 2000. Remote Sensing and Images Interpretation. 4th ed. New York: John Wiley & Sons.

Lunetta, R.S & Balogn, M.E. 1999. Application of Multi-Temporal Landsat 5 TM Imagery for Wetland Identification. *Photogrammetric Engineering & Remote Sensing.* 65:1303-1310.

Mather, Paul. (1999). Computer Processing of Remotely Sensed Images: An Introduction. John Wiley & Sons.

Microimages. 2001. Getting Started. Analysing Hyperspectral Images. [Online]. www.microimages.de/support/tutorial/hyprspec.pdf. [30.3.2003].

Munro, D.C & Touron, H. 1996. Estimation of Marshland Degradation in Southern Iraq using Multitemporal Landsat Images. Presented at the Eleventh Thematic Conference and Workshops on Applied Geological Remote Sensing, Las Vegas, Nevada.

National Water Act. 1998. Act No. 36 of 1998. Government Gazette Vol. 398, Cape Town.

Research Systems, Inc. 2001. ENVI User's Guide. Boulder: Research Systems, Inc.

SA Yearbook 2003/04, Published by Government Communications (GCIS)

Sabins, F. F. 1997. Remote Sensing. Principles and Interpretation. 3rd ed. New York: W. H. Freeman and Company.

Saraf, A.K., Goyal, V. C., Negi, A. S., Roy, B. & Choudhary, P. R. 2000. Remote Sensing and GIS techniques for the study of springs in a watershed in Garhwal in the Himalayas, India. *International Journal of Remote Sensing.* 21:2353-2361.

Schultz, R. E., Maharaj, M., Lynch, S. D., Howe, B. I. & Melvil-Thomson, B. 2002. South African Atlas of Agrohydrology and Climatology. Data on CD ROM.

Smith, J.H, Wickham, J.D, Stehman, S.V. & Yang, L. 2002. Impacts of Patch Size and Land-Cover Heterogenity on Thematic Image Classification Accuracy. *Photogrammetric Engineering & Remote Sensing.* 68: 65 - 70.

Statistics South Africa. 2001. Selected 1996 Census Data by Electoral Ward (With Maps). Data on CD Rom.

Stein A., van der Meer, F., Gorte, B. 1999. Spatial Statistics for Remote Sensing. Dordrecht: Kluwer Academic Publishers.

Thompson, M. 1996. A Standard Land-cover Classification Scheme for Remote Sensing Applications in South Africa. *South African Journal of Science.* 92:34-42.

Thompson, M, Marneweck G, Bell S, Kotze D, Muller J, Cox D and Smith R, 2002. A Methodology Proposed for a South African National Wetland Inventory. Prepared for Dept. Environment Affairs and Tourism by CSIR Environmentek. March 2002.

Townshend, J. R. G., Huang, C., Kalluri, S. N. V., Defries, R. S. & Liang, S. 2000. Beware of per-pixel characterization of land cover. *International Journal of Remote Sensing.* 21:839-843.

USGS. Landsat-7 Level-0 and Level-1 Data Sets Document. [Online]. Http://eosims.cr.gov:5725/DATASET_DOC/landsat7_dataset.html . [10.2.2002].

Van der Meer, F. D., de Jong, S.M. & Bakker, W. 2001. In van der Meer, F.D. & de Jong, S.M. (eds) *Imaging Spectrometry. Basic Principles and Prospective Applications,* pp38:61. Dordrecht: Kluwer Academic Publishers.

Vegter, J.R. 2001. Groundwater Development in South Africa and an Introduction to the Hydrogeology of Groundwater Regions. Pretoria: Water Research Commission.

Whitman, D. Gubbels, T. & Powell, L. 1999. Spatial Interrelationships between Lake Elevations, Water Tables, and Sinkhole Occurrence in Central Florida: A GIS Approach. *Photogrammetric Engineering & Remote Sensing.* 65:1169-1178.

Woodford A. & Chevallier L, (2001). Regional characterisation and mapping of Karoo fractured aquifer systems. An Integrated Approach using a Geographic Information System and Digital Image Processing. Pretoria: Water Research Commission.

The World Commission on Dams. 2000. Dams and Development - A New Framework for Decision-making. The Report of the World Commission on Dams. London and Sterling, VA: Earthscan Publications Ltd.

Yuen, P. 1998. Tasseled Cap Transform: Breathing New Life into Old Applications. [Online]. http://www.imagingnotes.com/novdec98/novstory6.htm. [8.7.2002].

READING LIST

The following sources were consulted but not referred to in the text.

Alavi Panah,S.K.& Goossens,R. 2000. The Role of TM Thermal band in describing the state/stress of vegetation. In Casanova, J.L. (ed.) *2000. Remote Sensing in the 21st Century: Economical and Environmental Applications*, pp31-36. Rotterdam: A.A. Balkema.

Babiker, M. 2000. Assessment of water resources in arid land using remote sensing. A case study from Sinka: District, Red Sea Hills, Sudan. 28th International Symposium on Remote Sensing of Environment, Cape Town.

Bailly, M.E. & Halls, H. C. 2000. Use of Remote Sensing Data to Locate Groundwater Trapped by Dykes in Precambrian Basement Terrains. *CANADIAN Journal of Remote Sensing*. 26:111-119.

Banoeng-Yakubo, B.K & Skjernaa, L. 2000. Application of remote sensing and geographical information system to hydrogeological studies in the Upper West Region Ghana. In Sililo O et al. (eds). Proceedings of the XXXIAH Congress on Groundwater: Past Achievements and Future Challenges, pp73-79. Rotterdam: A.A. Balkema.

Barrette, J., August, P & Golet, F. 2000. Accuracy Assessment of Wetland Boundary Delineation Using Aerial Photography and Digital Orthophotography. *Photogrammetric Engineering and Remote Sensing*. 66:409-416.

Basson, M.S. 1997. *Overview of Water Resources availability and utilization in South Africa.* Pretoria. Department of Water Affairs and Forestry.

Botha, J.F., Verwey,J.P., Van der Voort, I., Vivier, J.J.P., Colliston, W.P. & Lock, J.C. 1998. *Karoo aquifers. Their geology, geometry and physical behaviour. WRC report No 48 1 98.* Pretoria: Water Research Commission.

Braune, E. 2000. Towards a comprehensive groundwater resource management in South Africa. In Sililo O et al. (eds). Proceedings of the XXXIAH Congress on Groundwater: Past Achievements and Future Challenges, pp73-79. Rotterdam: A.A. Balkema.

Das, D. 1991. Extraction of Geomorphic and Geologic Information for Groundwater Exploration through Satellite Remote Sensing in and Around the Wachita Mountains, Oklahoma. Presented at the Eighth Thematic conference on Geologic Remote Sensing, Denver, Colorado.

Department of Water Affairs and Forestry. 1999. Resource Directed Measures for Protection of Water Resources: Wetland Ecosystems. Pretoria: Department of Water Affairs and Forestry.

Dini, J. 2003. South Africa: uKhahlamba Drakensberg Park and the National Wetlands Inventory. Dini, J. 2003. South Africa: uKhahlamba Drakensberg Park and the National Wetlands Inventory. [Online]. http://sedac.ciesin.org/ramsardg/casestudies/s_africa.html. [12.5.2003].

Dwivedi, R. S. & Sreenivas, K. 2002. The Vegetation and Waterlogging Dynamics as derived from Spaceborne Multi-spectral and Multitemporal Data. *International Journal of Remote Sensing*. 23 2729-2740.

Engman, E.T. & Gurney, R.J. 1991. Remote Sensing in Hydrology. London: Chapman & Hall.

Helmschrot, J. 2000. Application of Remote Sensing Data for Distributed Hydrological Model Parameterization of Large Scale Afforested Areas in the North East Cape Province (NECP), South Africa 28th International Symposium on Remote Sensing of Environment, Cape Town. Proceedings on CD ROM.

Hochschild V. (2000) Hydrological modeling of the Limpopo River Basin (Southern Africa). The input from Remote Sensing. 28th International Symposium on Remote Sensing of Environment, Cape Town. Proceedings on CD ROM.

Houhoulis, P. F. & Michener, W. K. 2000. Detecting Wetland Change: A Rule-Based Approach Using NWI and SPOT_XS Data. *Photogrammetric Engineering and Remote Sensing*. 66:205-211.

Huang, C., Wylie, B., Yang, L., Homer, C. & Zylstra, G. 2002. Derivation of a Tasseled Cap Transformation based on Landsat 7 At-Satellite Reflectance. U.S. Geological Survey. [Online]. http://landcover.usgs.gov/pdf/tesseled.pdf. [8.7.2002].

Kellgren, N & Sanders, P. 2000. Benefits of incorporating remote sensing techniques as a methodological approach for improved borehole siting in fractured rock. In Sililo O et al. (eds). Proceedings of the XXXIAH Congress on Groundwater: Past Achievements and Future Challenges, pp73-79. Rotterdam: A.A. Balkema.

Koeln, G. & Bissonnette, J. 2003. Cross-Correlation Analysis: Mapping Landcover Changes with a Historic Landcover Database and a Recent, Single-Date, Multi-spectral Image. [Online]. http://www.glc.org/wetlands/docs/CCA_Paper.doc. [20.7.2003].

Kok, T.S. 1992. Recharge of springs in South Africa. Department of Water Affairs Technical Report, GH 3748. Pretoria: Department of Water Affairs.

Krishnamurthy, J., Mani, A., Jayaraman, V. & Manivel, M. 2000. Groundwater resources development in hard rock terrain - an approach using remote sensing and GIS techniques. *JAG*. 2:204-215.

Musa, K. A., Akhir, J. M. & Abdullah, I. 2000. Groundwater Prediction Potential Zone in Langat Basin using the Integration of Remote Sensing and GIS. [Online]. http://gisdevelopment.net/aars/acrs/2000/ps3/ps318.shtml. [14.7.2003].

Pillay, D.L. 2001. An exercise to map wetlands in the Umgeni Catchment in Kwa-Zulu Natal using Landsat7 and other datasets. The Fourth Biennial International Conference of the Society of South African Geographers, Goudini Spa. Proceedings on CD ROM.

Rennies Wetlands Project. 2003. De-mystifying the Ramsar Convention. [Online]. http://psybergate.com/wetfix/Press/Press9/press.htm. [12.5.2003].

Sandholt, I., Rasmussen, K. & Andersen, J. 2002. A simple interpretation of the surface temperature/ vegetation index space for assessment of surface moisture status. Remote Sensing of Environment. 79:213-224.

Skirvin, S.M. 1991. Use of Processed Landsat Thematic Mapper Data to detect Surface Soil Moisture over Mountain Pediments, South Eastern Arizona. Presented at the Eighth Thematic conference on Geologic Remote Sensing, Denver, Colorado.

Smit, G.J. 1995. Research: Guidelines for Planning and Documentation. Halfway House: Southern Book Publishers.

Sustainable Development Department of the FAO: Food and Agriculture Organisation of the United Nations.Remote Sensing for Decision-makers. Groundwater exploration. Pilot Study in the Syrian Arab Republic. [Online]. http://www.fao.org/sd/EIdirect/EIre0070.htm. [10.2.2002].

Theseira, M.A., Thomas, G. & Sannier, C.A.D. 2002. An evaluation of spectral mixing modelling applied to a semi-arid environment. *International Journal of Remote Sensing*. 23:687-700.

University of Kentucky. Breaking into the Earth's Water Vault. [Online]. Http://www.rgs.uky.edu/ca/odyssey/spring01/water.html. [10.2.2002].

Van der Meer, F. D. & de Jong, S. M. (eds). Imaging Spectrometry. Basic Principles and Prospective Applications. Dordrecht: Kluwer Academic Publishers.

Zhang, J. & Goodchild, M. 2002. Uncertainty in Geographical Information. Bodmin: MPG Books Ltd.

APPENDIX A

BASIC PRINCIPLES OF REMOTE SENSING

Numerous definitions have been found in the literature for remote sensing. Campbell (1996) defines remote sensing as: "the practice of deriving information about the earth's land and water surfaces using images acquired from an overhead perspective, using electromagnetic radiation in one or more regions of the electromagnetic spectrum, reflected or emitted from the earth's surface."

Campbell (1996), Mather (1999) and Lillesand & Kiefer (2000) all give excellent introductions to the concepts of remote sensing. The following discussion is adapted from their texts.

Electromagnetic radiation/energy (EMR) is generated by several mechanisms, including changes in the energy level of electrons, acceleration of electrical charges, decay of radioactive substances, and the thermal motion of atoms and molecules. Nuclear reactions within the sun produce a full spectrum of EMR, which is transmitted through space without experiencing major changes. As this radiation approaches the earth, it passes through the atmosphere before reaching the earth's surface. However, oxygen, carbon dioxide and water vapour present in the atmosphere, all absorb different ranges of wavelengths more or less completely. This means that only some of the continuum of electromagnetic radiation can be used for remote sensing of materials at the earth's surface. These "block-outs" are known as atmospheric windows. Other atmospheric interactions further restrict what is possible. Clouds prevent all radiation, with the exception of wavelengths in the microwave region, from reaching the earth's surface. The presence of molecules of oxygen, nitrogen, water vapour and dust particles cause scattering which produces haze in the visible wavelengths. Refraction (the bending of light), occurs as EMR passes through atmospheric layers of varied clarity, humidity, and temperature. These atmospheric effects may have a substantial impact on the quality of images and the data generated by sensors, so it is important to understand these interactions.

As EMR reaches the earth's surface, it is reflected, absorbed or transmitted. Reflection occurs when a ray of light is redirected as it strikes a non-transparent surface. The nature of the reflection depends upon the size of surface irregularities in relation to the wavelength of the radiation considered. If the surface is smooth relative to wavelength, specular reflection occurs, whereby almost all incident radiation is redirected in a single direction. If a surface is rough relative to wavelength, diffuse or isotropic reflection occurs. In this case, energy is scattered more or less equally in all directions. Transmission of radiation occurs when radiation passes through a substance without significant attenuation (reduction in intensity). Water bodies are an example of good transmitter of EMR, and leaves of plants transmit significant amounts of radiation in the infrared wavelengths.

A fundamental premise in remote sensing is that we can learn about objects and features on the earth's surface by studying the radiation reflected and/or emitted by these features. A set of observations or measurements observed over a range of wavelengths, constitutes a spectral response pattern, also known as a spectral signature. Wolff, 1965 in Campbell (1996) states: "Everything in nature has its own distribution of reflected, emitted and absorbed radiation. These spectral characteristics can - if ingeniously exploited - be used to distinguish one thing from another or to obtain information about shape, size and other physical and chemical properties".

APPENDIX B

LANDSAT AND ASTER IMAGERY

Since the 1960s a very large number of satellites have been launched. For this research, data from two different sensors was used (Landsat and ASTER), and thus only these two will be discussed. Both Landsat and ASTER imagery can be ordered via the Internet and there is extensive information regarding these sensors available on these sites. Most introductory texts to remote sensing dedicate a chapter to describing the available sensors. However, as ASTER was only recently launched, only electronic texts on ASTER were found in the literature.

The Earth Resources Technology Satellite (ERTS) Program launched the first of a series of satellites (ERTS1) in 1972. Part of the National Aeronautics and Space Administration's (NASA) Earth Resources Survey Program, the ERTS programme and ERTS satellites were later renamed Landsat. This was to better represent the civil satellite program's prime emphasis on remote sensing of land resources. The latest satellite, Landsat7 was launched on 15 April 1999. This satellite carried the enhanced thematic mapper plus (ETM+). ETM+ is an enhanced version of the thematic mapper (TM) sensor flown aboard the previous landsat4 and -5 satellites. Sensor enhancements include the addition of the panchromatic band and two ranges, improved spatial resolution for the thermal band and two solar calibrators. (USGS, 2002)

Aster (Advanced Spacebourne Thermal Emission and Reflection Radiometer) is an imaging instrument that is flying on Terra, a satellite launched in December 1999 as part of NASA's Earth Observing System (EOS). Aster will be used to obtain detailed maps of land surface temperature, emmissivity, reflectance and elevation. The EOS platforms are part of NASA's Earth Science Enterprise, whose goal is to obtain a better understanding of the interactions between the biosphere, hydrosphere, lithosphere and atmosphere. The ASTER instrument was built in Japan for the Japanese Ministry of Economy, Trade and industry. A joint United States/Japan team is responsible for instrument design, calibration and validation. (California Institute of Technology, 2002)

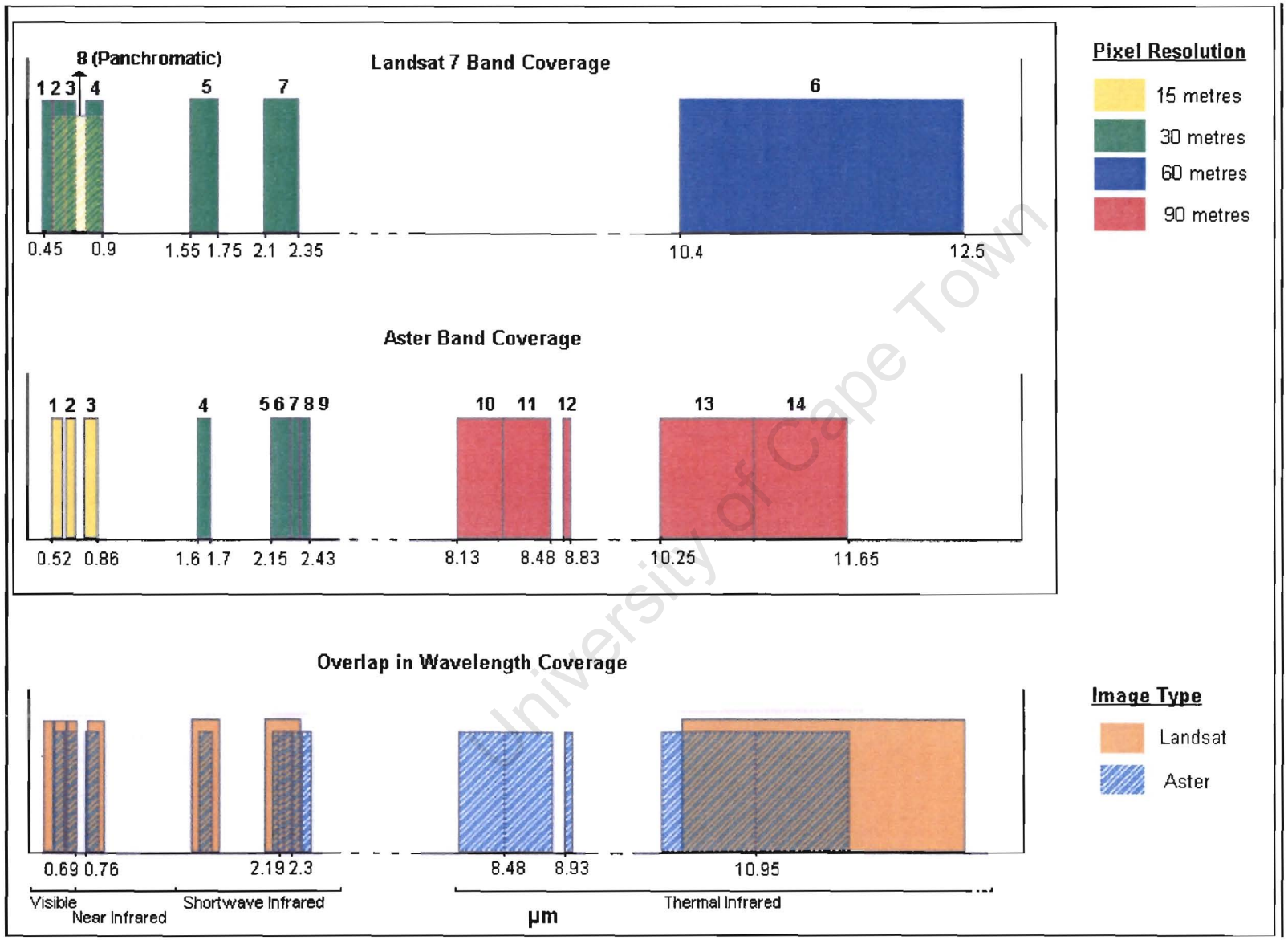

Figure B.1: Characteristics of Landsat and Aster Imagery

APPENDIX C

ADVANTAGES AND DISADVANTAGES OF SUPERVISED AND UNSUPERVISED CLASSIFICATION

Campbell (1996) highlights the advantages and disadvantages of both supervised and unsupervised classification as follows:

Unsupervised classification:

Advantages: *No extensive prior knowledge of the region is required.* However, this does not mean that the analyst can be completely ignorant of his or her study area as the classes resulting from the classification need to be allocated meaningful class names post classification.

The opportunity for human error is minimized. Many of the detailed decisions required in supervised classification are not required for unsupervised classifications so user bias is excluded. If the analyst has inaccurate perceptions of his or her study area, he or she will have little opportunity to influence the outcome of the classification.

Unique classes are recognized as distinct units.

Small classes which would otherwise be overlooked in supervised classification and included in other larger classes are maintained when running an unsupervised classification.

Disadvantages: *Classes identified by the classification do not necessarily match true land use covers.* Unsupervised classification identifies spectrally homogeneous classes within the data. These classes are not necessarily of use to the analyst and the analyst may have difficulty in matching the classes produced by the classification to the classes of interest required by the project.

Temporal changes cause loss in relationship between resulting classes from classification and real land use classes. Spectral properties of a scene change over time. This results in a fluctuating relationship between spectral classes and land use classes. The implications are that relationships defined for one image can seldom be defined for another.

Analyst has limited control. The analyst has very limited control over the menu of classes and their specific identities. This means that the results of a classification can seldom be matched to results in an adjacent region or at a different date.

Supervised classification:

Advantages: *User defined classes.* The analyst has control over which land cover classes he or she wishes to classify. This can be vitally important for time series analyses or where the classification needs to be compared to a classification from a different region.

Classes are always known. The analyst knows exactly which land cover classes he is attempting to map so is not left with the problem of trying to map classes with land cover types.

Error detection is simplified. The analyst can easily have an idea of the accuracy of the classification by checking to see whether the training data has been correctly classified.

Disadvantages: *Classification structure imposed on the data.* The classes selected by the analyst may not match the natural classes contained in the data. As a result, these classes may not be clearly defined in multi-dimensional space.

Poor training data. Training data are often focused on information properties rather than spectral properties. For example, a training region which is 100 % water body may have a different spectral response within the training area due to difference in water depth, turbidity etc.

Training data may not represent conditions throughout the image. This could be due to the fact that the image is very large, complex or some areas are inaccessible therefore lack of ground data exists.

Unique or small categories may be neglected due to the fact that they are unknown to the analyst or they represent a very small area of the image.

APPENDIX D

PARAMETERS USED IN THE ISODATA CLASSIFICATION

Number of classes: minimum 5, maximum 20;

Maximum number of iterations: 99

Change threshold %: 5

Minimum no of pixels in a class: 5

Maximum class standard deviation: 1

Minimum class distance: 5

Maximum number of merged pairs: 2

LANDSAT 7 TRUE COL

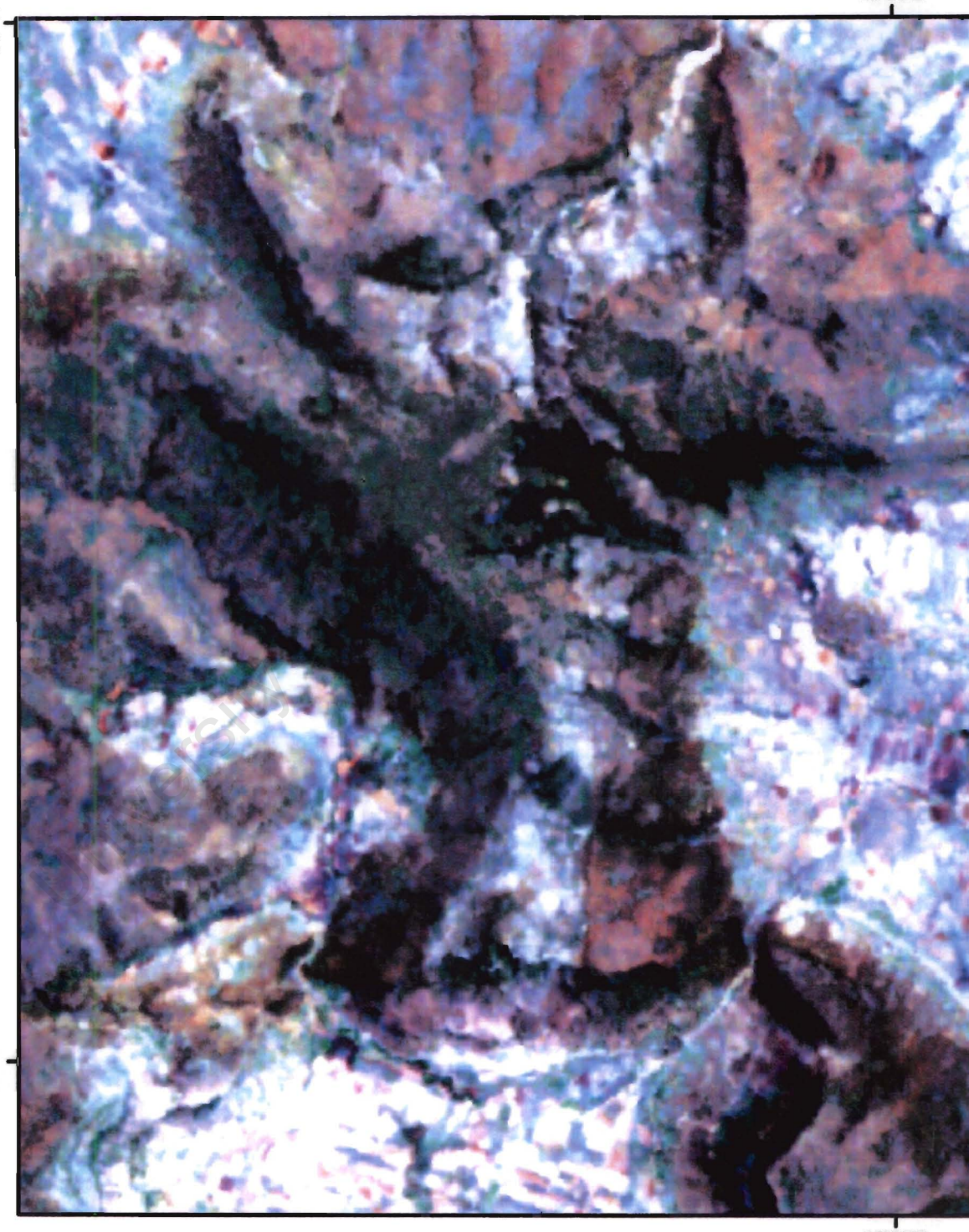

Image Acquisition date:
20 November 2000

Red = Band 3
Green = Band 2
Blue = Band 1

0 1

OUR IMAGE OF THE STUDY AREA

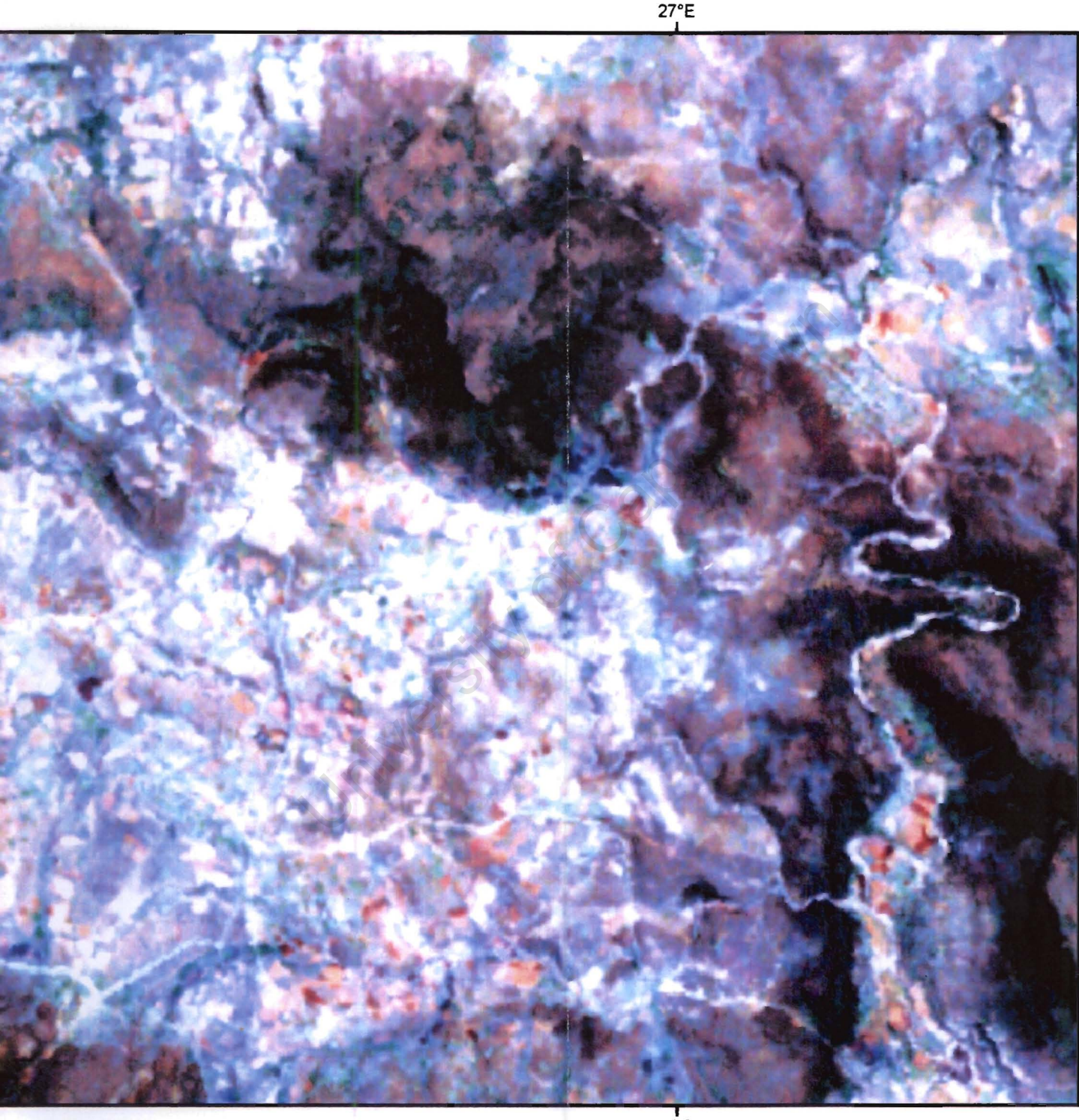

2 3 4 Kilometres

1 : 55 000

N
W E
S

Map Information:

Reference Spheroid: WGS84
Projection: UTM Zone 35 South

ASTER FALSE COLOU

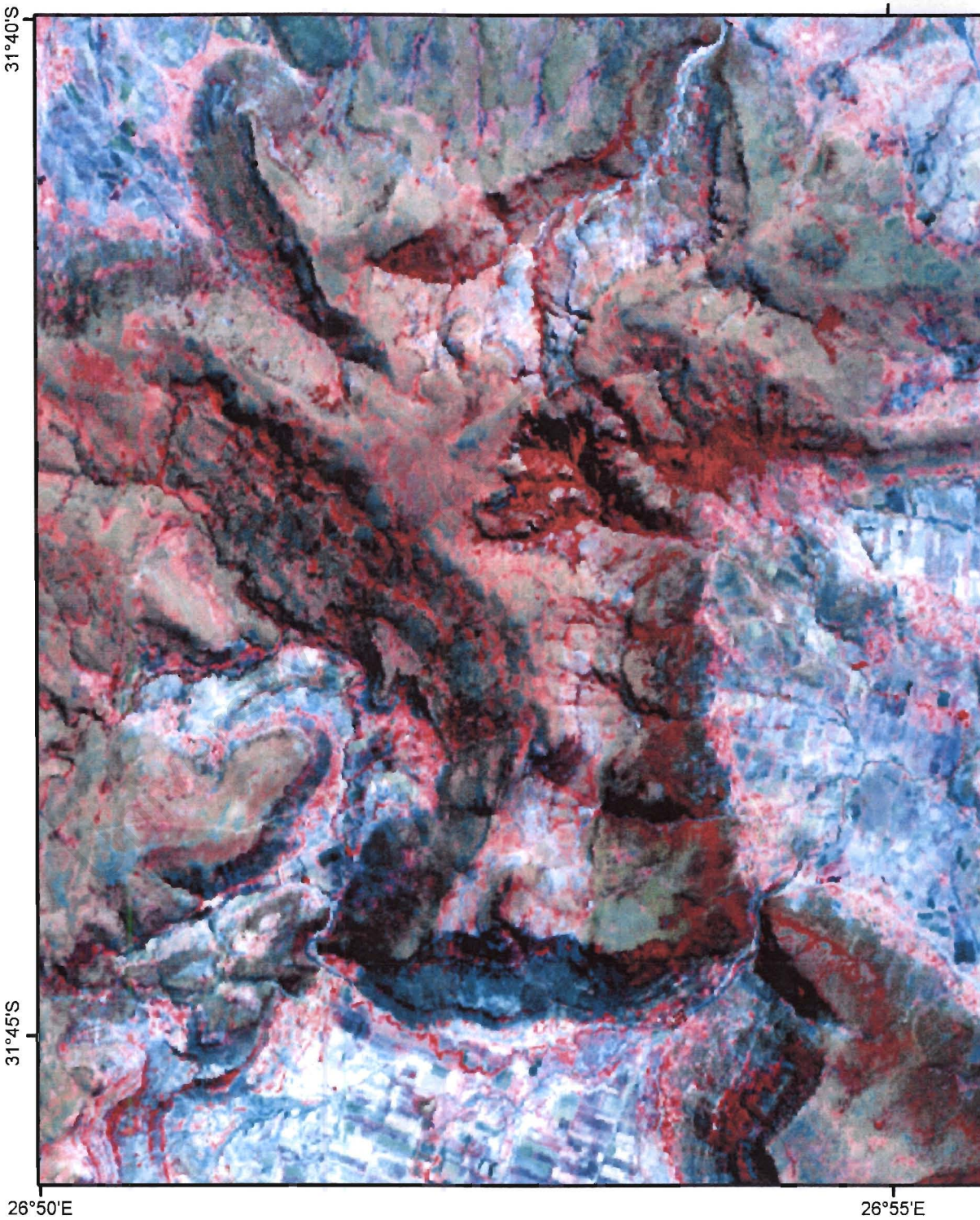

Image Acquisition Date:
16 October 2000

Red = Band 3
Green = Band 2
Blue = Band 1

0 1

IMAGE OF THE STUDY AREA

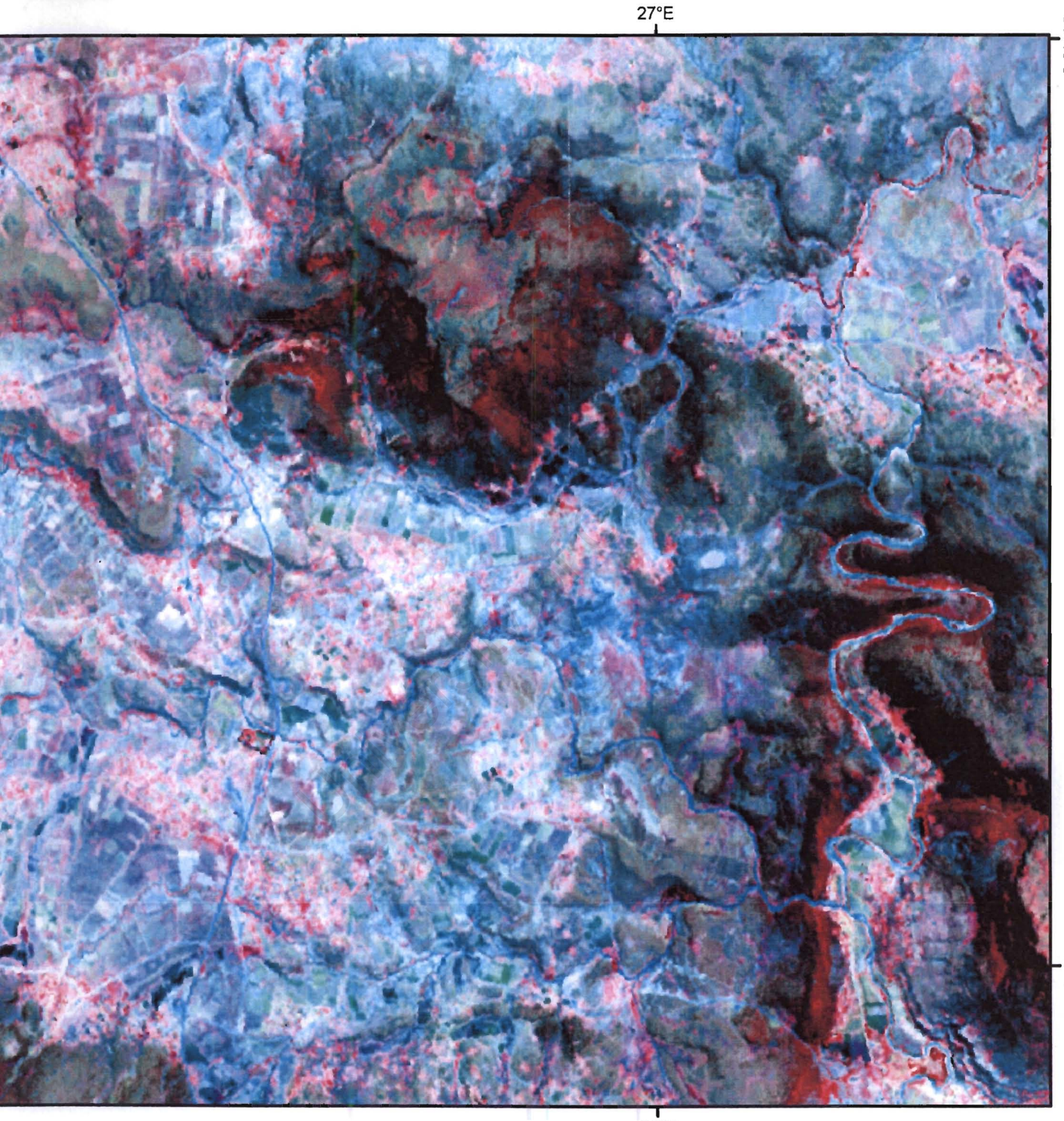

2 3 4 Kilometres

1 : 55 000

N
W E
S

Map Information:

Reference Spheroid: WGS84
Projection: UTM Zone 35 South